Research paper

# Composition of the gut microbiota transcends genetic determinants of malaria infection severity and influences pregnancy outcome

Catherine D. Morffy Smith [a], Minghao Gong [b], Alicer K. Andrew [a], Brittany N. Russ [b], Yong Ge [b], Mojgan Zadeh [b], Caitlin A. Cooper [a], Mansour Mohamadzadeh [b], Julie M. Moore [a,*,1]

[a] Department of Infectious Diseases and the Center for Tropical and Emerging Global Diseases, University of Georgia, Athens, GA, United States
[b] Department of Infectious Diseases and Immunology, University of Florida, Gainesville, FL, United States

A B S T R A C T

Background: Malaria infection in pregnancy is a major cause of maternal and foetal morbidity and mortality worldwide. Mouse models for gestational malaria allow for the exploration of the mechanisms linking maternal malaria infection and poor pregnancy outcomes in a tractable model system. The composition of the gut microbiota has been shown to influence susceptibility to malaria infection in inbred virgin mice. In this study, we explore the ability of the gut microbiota to modulate malaria infection severity in pregnant outbred Swiss Webster mice.
Methods: In Swiss Webster mice, the composition of the gut microbiota was altered by disrupting the native gut microbes through broad-spectrum antibiotic treatment, followed by the administration of a faecal microbiota transplant derived from mice possessing gut microbes reported previously to confer susceptibility or resistance to malaria. Female mice were infected with *P. chabaudi chabaudi* AS in early gestation, and the progression of infection and pregnancy were tracked throughout gestation. To assess the impact of maternal infection on foetal outcomes, dams were sacrificed at term to assess foetal size and viability. Alternatively, pups were delivered by caesarean section and fostered to assess neonatal survival and pre-weaning growth in the absence of maternal morbidity. A group of dams was also euthanized at mid-gestation to assess infection and pregnancy outcomes.
Findings: Susceptibility to infection varied significantly as a function of source of transplanted gut microbes. Parasite burden was negatively correlated with the abundance of five specific OTUs, including *Akkermansia muciniphila* and OTUs classified as *Allobaculum*, *Lactobacillus*, and S24-7 species. Reduced parasite burden was associated with reduced maternal morbidity and improved pregnancy outcomes. Pups produced by dams with high parasite burdens displayed a significant reduction in survival in the first days of life relative to those from malaria-resistant dams when placed with foster dams. At midgestation, plasma cytokine levels were similar across all groups, but expression of IFNγ in the conceptus was elevated in infected dams, and IL-10 only in susceptible dams. In the latter, transcriptional and microscopic evidence of monocytic infiltration was observed with high density infection; likewise, accumulation of malaria haemozoin was enhanced in this group. These responses, combined with reduced vascularization of the placenta in this group, may contribute to poor pregnancy outcomes. Thus, high maternal parasite burden and associated maternal responses, potentially dictated by the gut microbial community, negatively impacts term foetal health and survival in the early postnatal period.
Interpretation: The composition of the gut microbiota in *Plasmodium chabaudi chabaudi* AS-infected pregnant Swiss Webster mice transcends the outbred genetics of the Swiss Webster mouse stock as a determinant of malaria infection severity, subsequently influencing pregnancy outcomes in malaria-exposed progeny.
Fund: Research reported in this manuscript was supported by the University of Florida College of Veterinary Medicine (JMM, MM, and MG), the National Institute of Allergy and Infectious Diseases, the National Institute of Diabetes and Digestive and Kidney Diseases, and the Eunice Kennedy Shriver National Institute of Child Health and Human Development of the National Institutes of Health under award numbers T32AI060546 (to CDMS), R01HD46860 and R21AI111242 (to JMM), and R01 DK109560 (to MM). MG was supported by Department of Infectious Diseases and Immunology and University of Florida graduate assistantships. AA was supported by the 2017–2019 Peach State LSAMP Bridge to the Doctorate Program at the University of Georgia (National Science Foundation, Award # 1702361). The content is solely the responsibility of the authors and does not necessarily represent official views of the Eunice Kennedy Shriver National Institute of Child Health and Human

---

* Corresponding author.
  E-mail address: juliemoore@ufl.edu (J.M. Moore).
[1] Current Institution: Department of Infectious Diseases and Immunology, University of Florida, Gainesville, FL, United States.

**Research in context**

*Evidence before this study*

PubMed searches conducted on December 9, 2018 with the search terms "gut microbiota and infection," "gut microbiota and malaria," and "gut microbiota and pregnancy" were used to identify reports and knowledge relevant to this study.

The gut microbiota plays a critical role in normal immunological development and activation. The absence of the gut microbiota in germ-free animals is associated with impaired immunological development, while gut microbiota dysbiosis is associated with increased susceptibility to infections or other disorders within the gut and throughout the body in animal and human populations. The immunomodulatory activity of the gut microbiota is both direct and indirect – host contact with microbes and host contact with microbial metabolites have both been demonstrated to influence host immunology. The composition of the gut microbiota can influence susceptibility of inbred mice to experimental malaria infection and studies have linked gut microbial community with malaria susceptibility in human populations, indicating that even the development of hematogenous infections may be influenced by the microbial communities of the gut. Moreover, it is clear that the maternal gut microbiota is a key source of gut microbes in offspring. Understanding the host mechanisms governing susceptibility to malaria infection in vulnerable human subpopulations, such as pregnant women and young children, may be critical for developing adjunctive antimalarial therapies in the context of increasing antimalarial drug resistance.

*Added value of this study*

This study indicates that the composition of the gut microbiota can modulate malaria infection severity in a genetically diverse population of mice and in pregnant animals. Furthermore, this study identifies specific gut microbial community members that predict relative susceptibility or resistance to malaria infection in outbred pregnant mice. Variable maternal malaria infection severity, as informed by the composition of the gut microbiota, is shown to significantly influence foetal and postnatal outcomes.

*Implications of all the available evidence*

Gut microbes may contribute to malaria infection severity in human populations, perhaps influencing pregnancy outcomes in malaria-infected pregnant women. Furthermore, the manipulation of the human gut microbiota may allow for the enhancement of endogenous anti-malarial responses.

## 1. Introduction

Malaria poses a tremendous threat to the millions of pregnant women at risk for acquiring *Plasmodium falciparum* infections each year. In 2015, approximately 9·5 million pregnant women would have been exposed to malaria infection in the absence of malaria control programs seeking to prevent gestational malaria [1,2]. In pregnant women, *P. falciparum* infection is associated with the sequestration of infected red blood cells (iRBCs) in the placenta [3]. The function of the parasitized placenta is compromised by inflammation, coagulation, and tissue damage induced by pathogen infection [4–9]. The extent to which normal placental mechanisms and processes are disrupted by infection is unknown; however, abnormalities in uteroplacental blood flow [10], amino acid transport [11,12], glucose transport [13,14], and autophagy [15] have been identified in malaria-infected placentae. As a result of these disruptions in normal placental function, gestational malaria is associated with poor birth outcomes, including low birth weight due to intrauterine growth restriction, or preterm delivery, abortion, and stillbirth [16–21]. Furthermore, maternal malaria infection profoundly impacts the postnatal health and survival of the infants. Malaria-associated low birth weight is estimated to have a fatality rate of 37·5% [22], and infants born to malaria-infected women are more susceptible to malaria in early life [23–25]. Thus, understanding the pathogenesis of malaria in pregnancy is critical for improving maternal and child health outcomes in malarious regions.

Mouse models are important for the study of gestational malaria because the dysfunctional mechanisms linking maternal malaria infection and poor birth outcomes are incompletely understood, stymieing efforts to reduce the impact of malaria infection on pregnant women and their babies. Different parasite-mouse combinations best recapitulate different features of gestational malaria. Many mouse models for malaria in pregnancy result in spontaneous abortion or stillbirth [26–32], outcomes that are rarely observed in malaria-infected pregnant women living in highly endemic areas [33–35], even with chronic infection [36,37]. For this reason, we have developed a novel model for transgestational malaria infection utilizing Swiss Webster mice infected with *Plasmodium chabaudi chabaudi* AS [*Morffy Smith, in review*]. Swiss Webster dams infected with *P. chabaudi chabaudi* AS on gestational day (GD) 0 carry their pregnancies to term and deliver live pups, allowing for the exploration of the impact of prolonged maternal malaria infection on postnatal outcomes [*Morffy Smith, in review*]. In addition to modelling live birth following malaria infection throughout pregnancy, the use of outbred mice allows this model to act as a bridge between completely homogenous inbred mouse populations and genetically diverse human populations. However, genetic traits are not the only determinants of malaria severity in experimentally infected mice. In inbred mice, the composition of the gut microbiota has been identified as a major determinant of susceptibility to malaria [38,39]. It has previously been demonstrated that vendor-associated communities of gut microbes confer susceptibility or resistance to infection with multiple murine malaria species [38,39]. However, the ability of the gut microbiota to inform the susceptibility of pregnant mice to malaria and subsequently impact foetal and postnatal outcomes has not been elucidated.

Remarkably, we report here that the composition of the gut microbiota supersedes the diverse genetics of the outbred Swiss Webster mouse stock as a determinant of susceptibility to murine malaria infection. We demonstrate how the manipulation of the gut microbiota in a cohort of mice sourced from a single vendor allows for the modulation of infection severity, as well as foetal and postnatal outcomes. Swiss Webster mice from the National Cancer Institute Mouse Repository (NCI) are highly susceptible to *P. chabaudi chabaudi* AS infection [*Morffy*

*Smith, in review*]. The alteration of the gut microbiota via antibiotic treatment and the administration of a faecal microbiota transplant consisting of faeces collected from Jackson Laboratory-sourced mice (FMT[JAX]), reported to display microbiota-mediated resistance to malaria [39], significantly impacted disease outcomes in Swiss Webster mice. Maternal infection was less severe in mice receiving a faecal microbiota transplant consisting of faeces collected from Jackson Laboratory-sourced mice following antibiotic treatment (ABX-FMT[JAX]), and postnatal survival was improved relative to antibiotic-treated mice reconstituted with endogenous gut microbes (ABX-FMT[NCI]). Thus, the modulation of the gut microbiota may serve as a potential therapeutic approach for mitigating malaria infection severity and pregnancy outcomes in *P. chabaudi chabaudi* AS-infected outbred Swiss Webster mice. We anticipate that this will expand the *P. chabaudi chabaudi* AS-Swiss Webster model for transgestational malaria infection [*Morffy Smith, in review*] by enabling the exploration of pregnancy outcomes following severe and moderate parasite burdens using the same parasite-mouse combination.

## 2. Materials & methods

### 2.1. Mice

Three-week-old and six- to seven-week old Swiss Webster female mice, five- to six-week-old Swiss Webster male mice, and sexually mature Swiss Webster mice of both sexes (Clr:CFW) were purchased from NCI (Fredrick, MD), a facility managed by Charles River Laboratory. Male and female C57BL/6 J mice were purchased from the Jackson Laboratory as breeder stock and replaced at least every ten generations. Because *Helicobacter* infection can impact fecundity [40], animals were housed in *Helicobacter* species and norovirus-free rooms and maintained under specific-pathogen-free conditions at the University of Georgia Coverdell Vivarium, a barrier facility. Mice were provided with food (Mouse Diet 20; PicoLab's catalogue # is 5053; St. Louis, MO) and water ad libitum. Mice were acclimated to a 14-hour light/10-hour dark cycle, and rooms were maintained at a temperature between 65 and 75 °F and humidity between 40 and 60%. All animal protocols were approved by the University of Georgia Institutional Animal Care and Use Committee.

### 2.2. Antibiotic treatment and faecal microbiota transplantation

To induce dysbiosis of the native gut microbiota, four-week-old female and six- to seven-week-old male mice were treated over a fourteen day period with a broad spectrum antibiotic cocktail consisting of 100 mg/kg ampicillin (Gold Biotechnology; St. Louis, MO), 100 mg/kg metronidazole (MP Biomedicals; Santa Ana, CA), 100 mg/kg neomycin sulphate (Gold Biotechnology; St. Louis, MO), and 50 mg/kg vancomycin hydrochloride (Gold Biotechnology; St. Louis, MO) in sterile water for four consecutive days and on alternate days thereafter, until nine doses of antibiotic had been administered (summarized in Supp. Fig. 1b) [41,42]. The antibiotic cocktail was compounded fresh daily to minimize the degradation of antibiotics in aqueous solution and administered by oral gavage to ensure that each mouse received the appropriate dose of each drug. Antibiotics were not provided in drinking water because mice find metronidazole unpalatable and may refuse water to the point of fatal dehydration [42]. Control animals were not antibiotic treated.

Faecal microbiota transplantation was performed on the three consecutive days immediately following the final antibiotic dose. Donor faeces were collected from sexually mature NCI-sourced Swiss Webster mice and Jackson Laboratory-lineage C57BL/6 J breeder pairs and administered to both antibiotic treated and untreated control mice. Faecal pellets were collected directly into autoclaved Eppendorf tubes as spontaneously produced. A faecal slurry was generated by homogenizing donor faecal pellets in sterile 1× phosphate-buffered saline (PBS) at a

concentration of 50 mg faeces per 1 ml PBS [43]. Undigested fibrous material was removed from the slurry by centrifugation (380 ×$g$, 30 s), and 200 μl of the resulting supernatant was administered to each recipient mouse by oral gavage. Following each antibiotic and faecal slurry treatment, mice were moved to clean cages with fresh bedding in an attempt to reduce coprophagy and the bias in environmental exposure introduced by the outgrowth of some types of bacteria in heavily soiled bedding [44]. Neither faecal donor nor faecal microbiota transplant recipients were fasted at any time during the experiment. Following the completion of faecal microbiota transplant, animals were not handled for at least ten days to allow mice to recover from the stress of the antibiotic-treatment and faecal microbiota transplant protocols.

Four groups of experimental females were produced by this treatment protocol. First, mice were randomly assigned to either antibiotic or untreated control treatment groups. Subsequently, antibiotic-free control animals were randomly assigned to receive faecal microbiota transplant consisting of NCI (FMT[NCI]) or Jackson Laboratory (FMT[JAX]) faeces, yielding the CTRL-FMT[NCI] and CTRL-FMT[JAX] experimental groups, respectively. Similarly, antibiotic-treated animals were randomly assigned to receive either FMT[NCI] or FMT[JAX], resulting in the creation of ABX-FMT[NCI] and ABX-FMT[JAX] experimental groups. The assignment of mice to each of the four possible treatment groups is summarized in Supp. Fig. 1a.

### 2.3. Gut microbiota analysis

All faecal samples were collected directly from individual mice into autoclaved Eppendorf tubes as spontaneously produced, snap frozen in liquid nitrogen, and stored at −80 °C. DNA was isolated from faecal samples using ZymoBIOMICS DNA Miniprep Kit (Zymo Research, Irvine, CA) and faecal DNA concentration quantified using Qubit dsDNA HS Assay Kit (Invitrogen).

To confirm that antibiotic treatment was efficacious and induced dysbiosis necessary to create a niche for transplanted gut microbes, faecal samples collected prior to initiation of antibiotic treatment and after treatment completion (but before faecal microbiotal transplantation; see Supp. Fig. 1b) were processed and subjected to quantitative PCR analysis to detect relative amounts of 16S rDNA. The copy number of faecal 16S rDNA was quantified by qPCR using SsoAdvanced Universal SYBR Green Supermix (Bio-Rad). A standard curve for 16S rDNA was generated using primers 16S-F (5′-AGGATTAGATACCCTGGTA-3′) and 16S-R (5′-CRRCACGAGCTGACGAC-3′) and templates amplified from *E. coli*. The total bacterial loads were determined by absolute quantification method based on the standard curve. For quantifying the specific microbes, qPCR was performed using following primers: 5′-GGTGTC GGCTTAAGTGCCAT-3′/5′-CGGACGTAAGGGCCGTGC-3′ for *Bacteroides-Prevotella-Porphyromonas*, 5′-CCCTTATTGTTAGTTGCCATCATT-3′/5′-ACTCGTTGTACTTCCCATTGT-3′ for *Enterococcus*, and 5′-AGCAGTAGG GAATCTTCCA-3′/5′-CACCGCTACACATGGAG-3′ for Lactobacilli. The relative abundance of gut microbes was determined by normalising $C_T$ values of these genes to the $C_T$ values of 16S rDNA amplified from the same samples. The resulting data (Supp. Fig. 2) confirm antibiotic efficacy.

To comprehensively analyse faecal microbiol communities, matched faecal pellets collected prior to the administration of the first antibiotic dose and from ABX-FMT[NCI] and ABX-FMT[JAX] mice ten to twelve days following the completion of faecal microbiota transplantation were processed for isolation of DNA as above. A 16S rDNA library was constructed and sequenced as previously described [45,46]. Briefly, DNA samples were amplified by pairs of MiSeq compatible primers, targeting the 16S rDNA V4-V5 region. The primer sequences were reported previously [45]. Amplicons were purified by Omega E.Z.N.A. Gel Extraction Kit (Omega Bio-Tek, Inc., Norcross, GA) and quantified by Qubit 2.0 Fluorometer (Invitrogen, Grand Island, NY) and Kapa SYBR Fast qPCR kit (Kapa Biosystems, Inc. Woburn, MA.) After pooling equal amounts of amplicons with 10% of Phix control, the library was

sequenced on an Illumina MiSeq (Illumina, Inc., San Diego, CA). Sequence analyses were performed using QIIME (v1.9.1) [47]. Briefly, FastQ files were jointed, de-multiplexed and sequence depth for each sample was quantified (summarized in Supp. Data File 1). The de-multiplexed samples were then subjected to QIIME's core diversity analysis. For the analysis of faecal microbiota prior to the treatments, sequence depth was set to 51,157 reads/sample for the subsequent analyses while sequence depth of 67,808 reads/sample was applied for the analyses of faecal microbiota at 7–10 days following the faecal microbial transplantation. Principle coordinate analysis was first performed to investigate the global differences of microbiota composition among samples and the results were plotted using Python (V2.7.14). Alpha diversity analyses including Chao's richness were also performed in QIIME. Taxa were filtered by linear discriminant analysis effect size (LEfSe) analyses with default criteria ($P < 0.05$ by Kruskal-Wallis test; linear discriminant analysis (LDA) score > 2) and plotted in a cladogram based on their phylogenetic relationship [48]. To identify potential microbial species associated with parasite burden over the course of infection, represented by parasitaemia area under the curve (AUC) values, rarefied count values of each operational taxonomic unit across all faecal samples were log2 transformed and subjected to pairwise Spearman correlation analyses to determine the relationships between operational taxonomic unit (OTU) abundance and parasite burden. Sixteen significantly correlated OTUs are presented as a heat map. All five of the OTUs with a significant negative correlation with parasite burden are presented, as well as the eleven OTUs with the strongest positive correlations with parasite burden. The complete database for correlation analysis results is provided as Supp. Data File 2.

### 2.4. Parasites, infection, and infection monitoring

The following reagent was obtained through BEI Resources Repository, NIAID, NIH: *Plasmodium chabaudi chabaudi*, Strain AS, MRA-741, contributed by David Walliker. Parasites were maintained as frozen stock according to BEI Resource Repository guidelines and amplified in A/J mice for the purposes of infecting experimental mice.

Gravid infected and uninfected mice were generated by pairing experimental females with sexually mature Swiss Webster stud males at least ten days after the completion of faecal microbiota transplant (Supp. Fig. 1b). All experimental female mice were paired with male mice with concordant faecal microbe exposures. CTRL-FMT[JAX] and ABX-FMT[JAX] experimental females were exclusively paired with ABX-FMT[JAX] stud males, while autologously transplanted CTRL-FMT[NCI] and ABX-FMT[NCI] experimental females were paired with unmanipulated NCI-sourced studs. For some experiments, unmanipulated NCI-sourced mice were used as a proxy for malaria-susceptible ABX-FMT[NCI] mice, as the progression of infection in NCI-sourced mice [*Morffy Smith, in review*] is indistinguishable from the course of infection observed in ABX-FMT[NCI] mice. Unmanipulated NCI-sourced females were also paired with unmanipulated NCI-sourced studs. Paired females were examined each morning for the presence of a copulatory plug, indicative of successful mating. The day a plug was detected was considered gestational day (GD) 0. Pairing was done over a period of up to eleven consecutive days to achieve successful mating; thus, a period of eleven to twenty-three days elapsed between the final faecal microbiotal transplant and initiation of the experimental phase of the work (See Supp. Fig. 1b). Mated females were randomized into infected and uninfected cohorts. Mated females were considered pregnant if they exhibited at least a 10% increase in body weight by GD 8.

Infections were initiated as previously described [28–30,49,50]. Briefly, mice were infected intravenously with $10^3$ iRBCs diluted in 200 μl of $1\times$ PBS per 20 g of body weight. Virgin infected mice were infected alongside gravid animals as controls. Gravid uninfected mice received an intravenous injection of 200 μl 1xPBS per 20 g of body weight to control for handling. Body weight and haematocrit were measured at the time of infection, experimental day (ED) 0. Thus, in gravid mice, GD

0 was also ED 0. Regardless of pregnancy status, animals were transitioned to a higher fat breeder chow (PicoLab Mouse Diet 205,058; St. Louis, MO) at GD/ED 0.

Infection and pregnancy progression were monitored by measuring peripheral parasitaemia, haematocrit, and body weight daily between GD/ED 6 and GD/ED 18. Peripheral parasitaemia was measured by flow cytometry as previously described [51]. A drop of blood was collected by tail snip [52]. Within 4 h of collection, blood was diluted 1:50 in normal saline, and stained with 2.5 μM SYTO 16 Green Florescent Nucleic Acid Stain (ThermoFisher Scientific; Waltham, MA) for 20 min at room temperature protected from light. Stained blood was diluted one to nine in normal saline and analysed using a CyAn ADP Flow Cytometer (Beckman Coulter; Brea, CA) within 4.5 h of collection. iRBCs were identified based on size and fluorescence intensity, and a stained sample of uninfected blood was included each day as an internal control. Parasitaemia is reported as the percentage of iRBCs in the peripheral blood.

### 2.5. Assessment of term foetal and postnatal outcomes

At GD/ED 18, gravid infected and uninfected CTRL-FMT[NCI], CTRL-FMT[JAX], ABX-FMT[NCI], and ABX-FMT[JAX] mice, as well as identically treated infected virgin controls, were anesthetized using 2·5% Tribromoethanol and sacrificed by cervical dislocation. The uteri of gravid mice were removed and dissected. Foetuses and resorptions were counted, and foetal viability was assessed by reactive movement to prodding with forceps. Viable pups and their placentae were individually weighed.

To evaluate postnatal fitness, we generated additional gravid infected and uninfected ABX-FMT[NCI] and ABX-FMT[JAX] mice for the production of malaria-exposed and unexposed progeny. Neonates were fostered such that this assessment could be performed in the absence of variable maternal morbidity, and to effectively isolate the effects of in utero exposures to unique maternal malaria responses and gut microbiota. At gestational term (GD 18), donor pups produced by donor infected and uninfected ABX-FMT[NCI] and ABX-FMT[JAX] dams were delivered by caesarean section, dissected out of the uterus, individually weighed, and massaged with cotton swabs until clean and fully resuscitated. Donor pups were considered fully resuscitated when they were breathing regularly, pink in colour, and displaying spontaneous wriggly movement. Fully resuscitated donor pups were mixed with the native litter of an uninfected, unmanipulated Swiss Webster foster dam. Native litters were zero to three days of age at the time of fostering. The foster dam's native pups received footpad tattoos using a nontoxic carbon pigment ink (Super Black Speedball India Ink; Statesville, NC) at the time of fostering so that they could be differentiated from fostered pups [53,54]. Litter size was capped at 15 pups, with a minimum of three native pups retained in the final litter. Following fostering, the cage was not disturbed for four days to maximize foster dam acceptance of the fostered pups. When the fostered pups were four days old, they were counted, individually identified by footpad tattooing [53,54], and individually weighed. Individual fostered pups were weighed every three days between four days of age and weaning at 22 days of age. Sex was determined visually at weaning.

### 2.6. Plasma and tissue collection at midgestation

Cohorts of malaria infected and uninfected ABX-FMT[JAX] and NCI-sourced dams were generated to assess immunological differences in the placental and peripheral environment in mice experiencing relatively low and high parasite burdens, respectively. Mice were sacrificed for plasma and tissue collection at GD/ED 10. Mice were anesthetized with 2·5% Tribromoethanol. Blood was collected by venepuncture of the caudal vena cava [55] using an Anticoagulant Citrate-Dextrose (ACD) charged syringe. Platelet-poor plasma was isolated by double centrifugation of whole blood containing 10% ACD v/v [56], frozen in

liquid nitrogen, and stored at −80 °C. Following blood collection, mice were euthanized by cervical dislocation. The uterus was removed and weighed. Well-vascularized embryos without haemorrhaging were considered viable. Viable embryos, nonviable embryos, and resorption scars were counted, with nonviable embryos and resorption scars included in the count of total embryos. Conceptuses were dissected from the uterus, snap frozen in liquid nitrogen, and stored at −80 °C prior to RNA isolation for gene expression analysis.

### 2.7. Peripheral cytokine titres

Plasma cytokine levels at midgestation were measured using the Bio-Plex Pro™ Mouse Cytokine Th17 Panel A 6-Plex kit (Bio-Rad; Hercules, CA), read using the Bio-Rad Bio-Plex® 200 system (Bio-Rad; Hercules, CA), and analysed with Bio-Plex Manager™ software (Bio-Rad; Hercules, CA).

### 2.8. Conceptus gene expression

GD/ED 10 conceptuses were homogenized in lysis buffer using the TissueMiser (Fisher Scientific; Waltham, MA) or Bullet Blender Gold (Next Advance; Troy, NY) prior to RNA isolation using the RNeasy Plus Mini Kit (Qiagen; Germantown, MD). Three or more conceptuses were pooled per dam. cDNA was subsequently synthesized using the High-Capacity cDNA Reverse Transcription Kit (Applied Biosystems; Foster City, CA). Relative mRNA abundance was determined using Power SYBR® Green Supermix (Applied Biosystems; Foster City, CA) and the C1000 Touch Thermal Cycler (cytokine-encoding genes and *Ubc*; CFX96 Real Time Systems, Bio-Rad, Hercules, CA) or the Roche Light Cycler 96 (genes encoding cell type markers and *Gapdh*; Roche, Indianapolis, IN). Samples were assayed in duplicate for all genes. Average threshold cycle (Ct) values for genes of interest were normalized to average *Ubc* or *Gapdh* Ct values. The expression of genes encoding cytokines were internally normalized to *Ubc* expression levels, while the expression of genes characteristic of leukocyte subsets was normalized to *Gapdh* expression levels. The ΔΔCt method was used to determine the relative transcript abundance of each gene of interest [57]. Gene expression in infected NCI-sourced, uninfected ABX-FMT$^{JAX}$, and infected ABX-FMT$^{JAX}$ mice is presented relative to the mean expression value in uninfected NCI-sourced mice. All primer sequences and amplicon sizes are listed in Supplementary Table 1.

### 2.9. Malarial pigment/haemozoin quantification and histopathology

Embryos were preserved within the uterus for histological analysis. Briefly, tissue was removed at sacrifice and fixed in 4% buffered formalin. A small amount of formalin was injected into the uterus to ensure complete penetration of the fixative. Tissues were dehydrated with ethanol, cleared in xylenes, and infiltrated in paraffin, and embedded. Seven μm sections were stained with haematoxylin and eosin, to assess histopathological features, or Giemsa, to assess haemozoin deposition. Haemozoin deposition in the placental junctional zone was measured using a Keyence BZ-X710 microscope with BZ-X Analyzer software. Using a 60× oil objective, images representing an area measuring 242 μm × 181 μm were captured across 3–5 individual placentae. Total space captured among ABX-FMT$^{JAX}$ mice measured 3,907,138 ± 1,426,561 μm$^2$ and in NCI-sourced mice, 4,134,909 ± 629,135 μm$^2$ (mean ± SD; $P > 0.05$). Using BZ-X analyzer software, acellular spaces, representing maternal blood space not occupied by cells, were excluded to allow calculation of tissue/cell area occupied by haemozoin, detected by hue. Haemozoin found in iRBCs, maternal proinflammatory cells, trophoblast, and fibrin was enumerated and percent area occupied calculated according to the formula: (area of haemozoin/total area assessed) x 100. Total acellular space, taken as a proxy for maternal blood spaces, was calculated by subtracting the total assessed space from the total captured space and was adjusted to a per image basis

by dividing by total image number. Any images having at least one prominent maternal blood canal were tallied.

### 2.10. Statistics

Descriptive statistical analyses were performed using GraphPad Prism 7 (GraphPad Software; La Jolla, California). All raw clinical data are presented as mean ± SEM. Error bars are not depicted if the error bars are shorter than the height of the symbol. AUC was calculated for the curves depicting parasitaemia, haematocrit, and percent starting weight between GD 0 and GD 18 for each mouse. Data are shown as scatter plots (with a bar or line representing the mean) or box and whisker plots with whiskers indicating the 10th and 90th percentiles and individual points denoting outliers. Proportions were compared using the two-tailed Fisher exact test. $P$ values ≤ 0.05 were considered statistically significant. Normally distributed data were analysed using parametric statistics and non-normally distributed data were analysed using nonparametric statistics, all with appropriate post-hoc tests for multiple comparisons as outlined in figure legends.

Mixed linear models analysis (SAS 9.4) was used to estimate differences in term foetal and placental weights as a function of dam infection severity, and postnatal pup growth as a function of dam treatment and infection severity. In both cases, the interrelatedness of pups born to the same dam was controlled with a random term for the dam. Best fit for the former model was obtained with the inclusion of antibiotic treatment (binary variable), faecal microbiota transplant group (binary variable), and parasitaemia AUC value (continuous variable); number of viable pups per dam, and interaction terms between antibiotic treatment status and faecal microbiota transplant group, parasitaemia AUC and faecal microbiota transplant group and parasitaemia AUC and antibiotic treatment status were tested but omitted as they did not improve model fit. The latter model assessed trends over time for changes in pup growth; repeated measures in the pups were accommodated with a repeat command and the relatedness of pups born to the same dam was accounted for with a random term for the dam. Model fitting revealed that the number of pups at weaning, and age at weight measurement, with associated interaction terms with the latter, influenced trends in weight gain. Maternal infection status and maternal treatment group were not significant in initial models but are depicted in the figure for illustration purposes.

## 3. Results

### 3.1. The composition of the gut microbiota is shaped by faecal microbiota transplantation following broad-spectrum antibiotic treatment

Faecal samples were collected from experimental mice prior to antibiotic treatment, following the completion of antibiotic treatment but prior to faecal microbiota transplantation, and ten to twelve days after the completion of antibiotic treatment and faecal microbiota transplant. Comparison of samples collected before antibiotic treatment to those collected after that treatment was completed confirmed that treatment significantly reduced overall bacterial load (Supp. Fig. 2a), with several specific bacterial genera being reduced to low or undetectable levels (Supp. Fig. 2b). As expected, such reductions were not evident in mice not treated with antibiotics (Supp. Fig. 2).

Samples collected prior to antibiotic treatment and post-faecal microbiota transplantation from animals that were later allocated to malaria-infected virgin or gravid cohorts were analysed to determine the impact of treatment on the composition of the gut microbiota. Global changes in the composition of the gut microbiota were determined by UniFrac analysis. Principle coordinate analysis revealed no separation between microbial communities collected from individual mice prior to treatment (Supp. Fig. 3a). Likewise, at this time point, mice that were ultimately allocated to both treatment groups possessed similar proportions of faecal microbes belonging to the dominant phyla

(Supp. Fig. 3d). Despite the shared origin and identical treatment of mice prior to the initiation of antibiotic treatment, mice that were later allocated to the ABX-FMT[NCI] treatment group exhibited reduced faecal microbial diversity, as indicated by significantly lower Chao1 richness, observed operational taxonomic units, and Shannon Index values compared to mice later allocated to the ABX-FMT[JAX] treatment group (Supp. Fig. 3b).

Following a rest period of ten to twelve days post-FMT, gut microbial communities from mice that received ABX-FMT[NCI] and ABX-FMT[JAX] clustered separately by principle coordinate analysis, indicating that antibiotic treatment followed by FMT[NCI] or FMT[JAX] administration resulted in distinct communities of gut microbes (Fig. 1a and Supp. Fig. 4). Reduced faecal microbial diversity was observed in mice that received ABX-FMT[JAX] relative to mice that received ABX-FMT[NCI], indicated by a significant reduction in Chao1 richness, observed operational taxonomic units, and Shannon Index values in ABX-FMT[JAX] recipients (Fig. 1b). By LEfSe analysis, some taxa, including Lactobacillaceae,

Rikenellaceae and Ruminococcaceae were enriched in ABX-FMT[NCI] mice, while Erysipelotrichaceae and Bacteroidaceae were enriched in ABX-FMT[JAX] mice (Fig. 1c).

The composition of the faecal microbiota was also evaluated in a group of antibiotic-treated FMT recipient mice sacrificed at GD/ED 18. These results show that FMT donor exerts a more significant influence on the composition of the gut microbiota than pregnancy status (Supp. Fig. 5).

### 3.2. Functional gut microbiota determines malaria infection severity in outbred Swiss Webster mice

In gravid and virgin Swiss Webster mice, the composition of the gut microbiota may determine susceptibility to malaria infection. On average, gravid infected ABX-FMT[NCI] mice achieved a peripheral peak parasitaemia of approximately 40% (Fig. 2a), consistent with the parasite burdens observed in unmanipulated Swiss Webster mice purchased
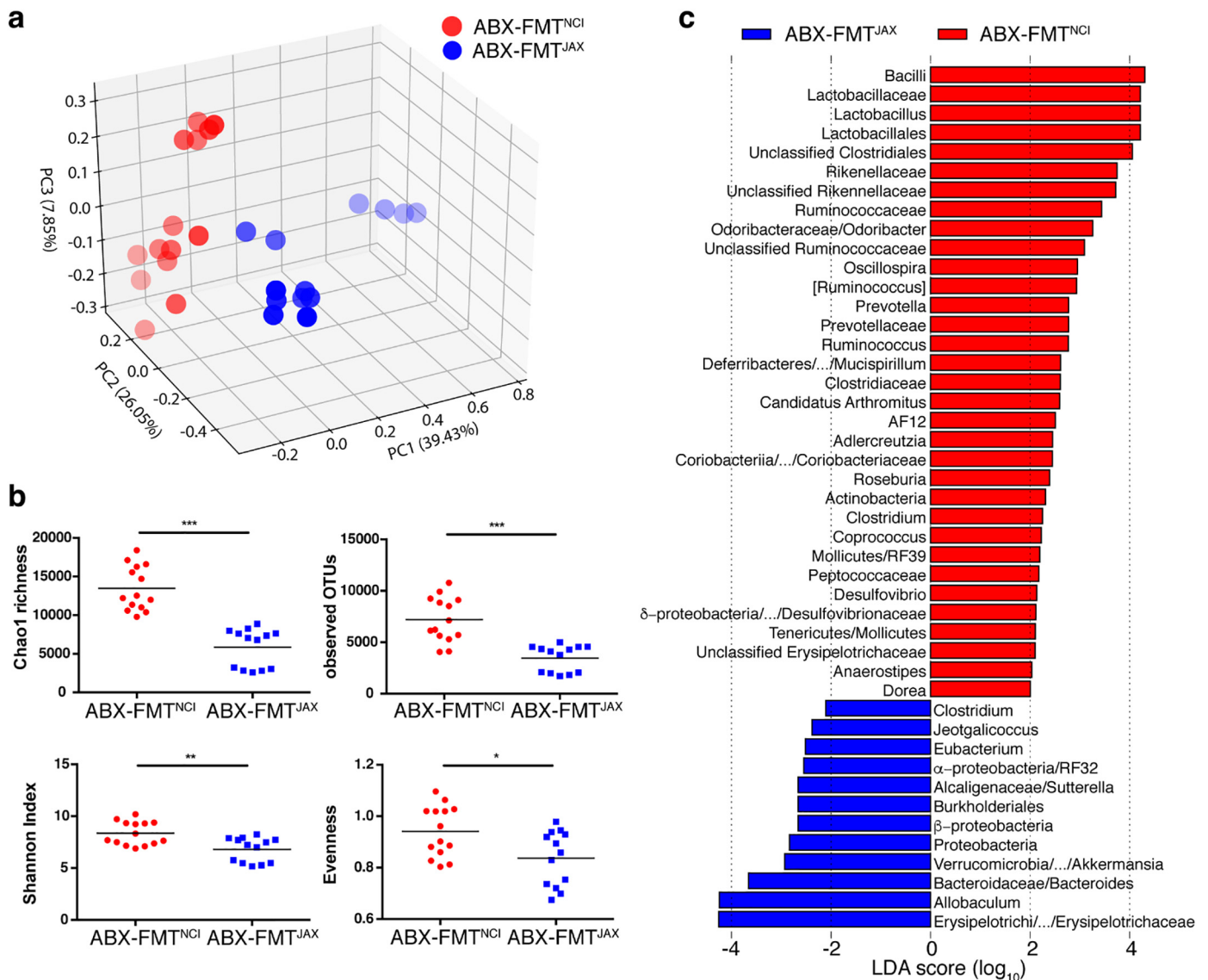


**Fig. 1.** Mice receiving ABX-FMT[NCI] and ABX-FMT[JAX] have distinct gut microbiota compositions. a) Three-dimensional plot of principal coordinate analysis (PCoA) of microbial communities in ABX-FMT[JAX] and ABX-FMT[NCI] mice approximately one week following the completion of FMT. Fainter colours correspond to points that are further from the page along the z-axis. b) Summary box plots of Chao1 richness, observed OTUs, Shannon Index, and Evenness. Significant differences in Chao1 richness ($t$-test, $P \leq 0.001$), observed OTUs ($t$-test, $P \leq 0.001$), Shannon Index ($t$-test, $P \leq 0.01$), and Evenness ($t$-test, $P \leq 0.05$) are observed between groups. c) Histogram of linear discriminant analysis (LDA) reveals the most differentially abundant taxa between faecal samples collected from ABX-FMT[JAX] and ABX-FMT[NCI] mice. Only taxa meeting the criteria ($P < 0.05$ by Kruskal-Wallis test; LDA score > 2) are shown. Different levels of taxa categorized in the same phylogenetic branch, with the same LDA scores, are collapsed in the same bar of which the highest and lowest levels are separated by slash and the middle levels are left out. *$P \leq 0.05$; **$P \leq 0.01$; ***$P \leq 0.001$.

from NCI [*Morffy Smith, in review*]. In contrast, gravid infected ABX-FMT^JAX mice achieved a peripheral peak parasitaemia of approximately 13% (Fig. 2a). Over the course of infection, a statistically significant reduction in parasite burden was observed in gravid infected ABX-FMT^JAX mice compared to gravid infected ABX-FMT^NCI mice (Fig. 2d).

Malaria infection was associated with the development of malarial anaemia in gravid ABX-FMT^NCI and ABX-FMT^JAX mice around the time of peak infection (Fig. 2b). A significant reduction in haematocrit was observed in both gravid infected ABX-FMT^NCI and ABX-FMT^JAX mice compared to uninfected controls (Fig. 2e). Over the course of infection, gravid infected ABX-FMT^NCI mice displayed a statistically significant reduction in haematocrit compared to gravid infected ABX-FMT^JAX mice (Fig. 2e), reflecting the higher parasite burdens observed in the former (Fig. 2d). In the absence of infection, treatment group did not significantly influence haematocrit over the course of the experiment (Fig. 2e).

Gestational weight change also reflected parasite burden. Gravid infected ABX-FMT^NCI mice displayed reduced weight gain between GD/EDs 9 and 11, corresponding with the time of peak infection (Fig. 2c).

This stasis in weight gain was not observed in gravid infected ABX-FMT^JAX animals or gravid uninfected controls (Fig. 2c). Although gravid infected ABX-FMT^NCI mice resumed weight gain at GD/ED 12, they did not fully recover relative to the other groups of gravid mice (Fig. 2f). Among gravid ABX-FMT^JAX animals, malaria infection was not associated with a statistically significant reduction in weight change over the course of gestation (Fig. 2f). Alterations in pregnancy-associated weight gain were not attributable to differences in weight at the start of the experiment (Supp. Fig. 6).

In the absence of antibiotic pretreatment, FMT source did not influence infection severity (Supp. Fig. 7). Gravid infected CTRL-FMT^NCI and CTRL-FMT^JAX mice developed similar parasite burdens over the course of gestation (Supp. Fig. 7d). Malaria infection was associated with a significant reduction in haematocrit over the course of gestation, but a significant difference in haematocrit was not observed between gravid infected CTRL-FMT^NCI and CTRL-FMT^JAX mice, reflecting the similar parasite burdens observed in these cohorts (Supp. Fig. 7e). No significant changes in body weight were observed over the course of gestation either as a function of treatment group or infection status (Supp.
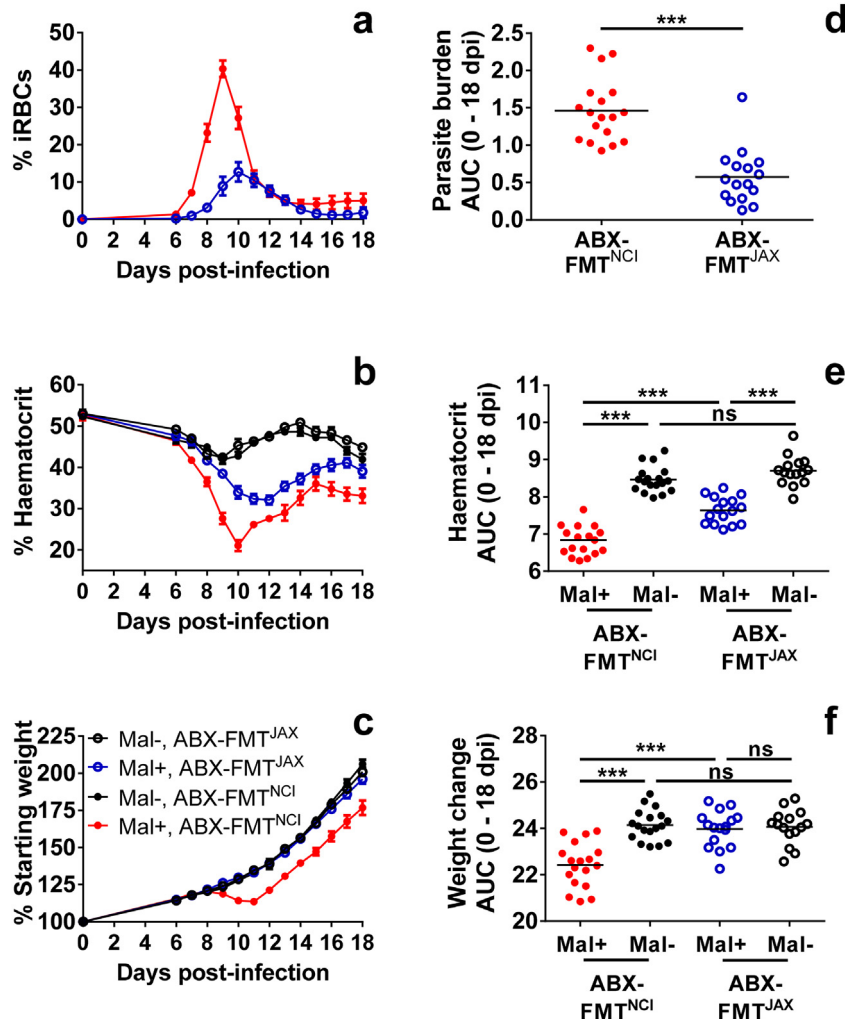


**Fig. 2.** Parasitaemia, haematocrit, and weight change in gravid ABX-FMT^NCI and ABX-FMT^JAX Swiss Webster mice. a) Parasitaemia in gravid infected (Mal+) ABX-FMT^NCI and ABX-FMT^JAX mice was estimated by flow cytometry and is presented as the percentage of iRBCs in the peripheral blood. b) Percent haematocrit was measured throughout infection in gravid Mal + mice and uninfected (Mal-) controls. c) Weight change in gravid Mal + mice and Mal- controls is presented as the percentage of body weight relative to 0 days post-infection or post-mock infection. d) Area under the curve (AUC) was calculated for the parasitaemia curve of each individual animal. A statistically significant difference in parasite burdens is observed between Mal + ABX-FMT^NCI and ABX-FMT^JAX dams (Mann Whitney test, $P < 0.001$). e) AUC was calculated for the haematocrit curve of each individual dam. Statistically significant differences in haematocrit are observed between Mal + and Mal- ABX-FMT^NCI dams ($P < 0.001$), between infected and uninfected ABX-FMT^JAX dams ($P < 0.001$), and between infected ABX-FMT^NCI and infected ABX-FMT^JAX dams ($P < 0.001$; one-way ANOVA with Bonferroni multiple group comparisons). f) AUC was calculated for the weight change curve of each individual animal. Statistically significant differences in weight change are observed between Mal + and Mal- ABX-FMT^NCI dams ($P < 0.001$), and between infected ABX-FMT^NCI and infected ABX-FMT^JAX dams ($P < 0.001$; one-way ANOVA with Bonferroni multiple group comparisons). Gravid Mal+, ABX-FMT^NCI $n = 18$; Gravid Mal-, ABX-FMT^NCI $n = 18$; Gravid Mal+, ABX-FMT^JAX $n = 16$; Gravid Mal-, ABX-FMT^JAX $n = 15$; *** $P \leq 0.001$; ns $P > 0.05$.

Fig. 7f). Treatment group did not significantly alter haematocrit or weight change in gravid uninfected mice (Supp. Fig. 7e, f) nor were body weights among the groups different at the time of infection (GD/ED 0; Supp. Fig. 6).

The results observed in virgin infected mice were similar to those seen in identically treated gravid infected mice, with ABX-FMT[JAX] have lower parasitaemia and less severe anaemia relative to ABX-FMT[NCI] mice (Supp. Fig. 8d, e). Unlike gravid mice, however, no significant change in weight was observed over the course of infection among the treatment groups (Supp. Fig. 8f).

### 3.3. Specific operational taxonomic units are correlated with parasite burden

To assess the extent to which specific members of the gut microbiota are associated with susceptibility to malaria infection, the Spearman correlation between the abundance of specific OTUs and parasite burden, represented by parasitaemia AUC, was determined. The five OTUs significantly negatively correlated with parasite burden and the 11 OTUs with the strongest significant positive correlations with parasite burden are depicted in Fig. 3.

Fifty-six OTUs were positively correlated with parasite burden (Supp. Data File 2). Of these OTUs, twenty-six were classified as S24-7 family members, of which the total relative abundances were not significantly different between the groups of mice. In addition, OTUs classified as members of the order Clostridiales, including members of the Lachnospiraceae and Ruminococcaceae families, were prominently represented within this group. Intriguingly, the OTU (New.ReferenceOTU1914) with the strongest positive correlation with parasite burden ($R = 0.866$, adjusted $p = 1.29\text{E-}06$) was unassigned. Among the ten OTUs with the next strongest positive correlations with parasite burden were OTUs classified as members of the genus *Adlercreutzia* (New.ReferenceOTU483), the genus *Lactobacillus* (OTU266445), the S24-7 family (New.ReferenceOTU423, New.ReferenceOTU616, New.ReferenceOTU1498), the Ruminococcaceae family (New.ReferenceOTU42, New.CleanUp.ReferenceOTU292001), the Lachnospiraceae family (New.ReferenceOTU1031), the Rikenellaceae family (New.ReferenceOTU1530), and the order Clostridiales (New.ReferenceOTU778). Consistent with these results, *Adlercreutzia* species, *Lactobacillus* species, Ruminococcaceae family members, and Rikenellaceae family members were found to be more abundant in ABX-FMT[NCI] faeces relative to ABX-FMT[JAX] faeces by LEfSe analysis (Fig. 1c).

Only five OTUs were significantly negatively associated with parasite burden; two classified as S24-7 family members (OTU214699 and OTU341448), one classified as *Allobaculum* (OTU277143), one classified as *Lactobacillus* (New.ReferenceOTU332), and one classified as *Akkermansia muciniphila* (OTU273232). Interestingly, while LEfSe analysis revealed the greater abundance of *Allobaculum* and *Akkermansia* species in ABX-FMT[JAX] faeces, *Lactobacillus* species were more highly represented in ABX-FMT[NCI] faeces (Fig. 1c).

### 3.4. Maternal infection severity influences foetal viability at gestational term

Dams were sacrificed on GD/ED 18 and uteri removed to count foetuses and assess foetal viability. Spontaneous midgestational pregnancy loss due to infection was observed in some dams. Of the dams sacrificed to assess foetal weight and viability at term, 9% (1/11) of gravid infected ABX-FMT[NCI] mice, 25% (2/8) of gravid infected CTRL-FMT[NCI] mice, and 29% (2/7) of gravid infected CTRL-FMT[JAX] mice did not have foetuses or resorptions in the uterus at term despite displaying weight gain consistent with pregnancy at GD 8. These mice were assumed to have suffered spontaneous pregnancy loss, expelling their embryos around the time of peak infection. Such mice were excluded from further analysis. No mated mice allocated to gravid infected ABX-FMT[JAX] or gravid uninfected cohorts failed to produce foetuses at term.

The mean numbers of total and viable foetuses produced by individual ABX-FMT[NCI] and ABX-FMT[JAX] dams did not differ significantly as a function of infection status or infection severity (Supp. Fig. 9a). However, in populations of foetuses pooled by maternal treatment group and infection status, lower parasite burdens were associated with improved foetal outcomes. Infected ABX-FMT[JAX] mice displayed a tendency towards higher foetal viability ($n = 10$ dams, 96/112 or 86% viability) relative to infected ABX-FMT[NCI] dams ($n = 11$ dams, 90/132 or 68% viability; $P = 0.0540$, two-tailed Fisher exact test). No significant difference in foetal viability was observed between treatment groups in the absence of infection. Uninfected ABX-FMT[JAX] mice produced a similar proportion of viable foetuses ($n = 10$ dams, 112/126 or 89% viability) as uninfected ABX-FMT[NCI] mice ($n = 9$ dams, 101/116 or 87% viability; $P = 0.6959$, two-tailed Fisher exact test), indicating that treatment itself did not impact foetal outcomes.

The mean numbers of total and viable foetuses produced by individual CTRL-FMT[NCI] and CTRL-FMT[JAX] dams did not differ significantly as a function of infection status or treatment group (Supp. Fig. 10a). When foetuses were pooled by dam group, no significant difference in foetal
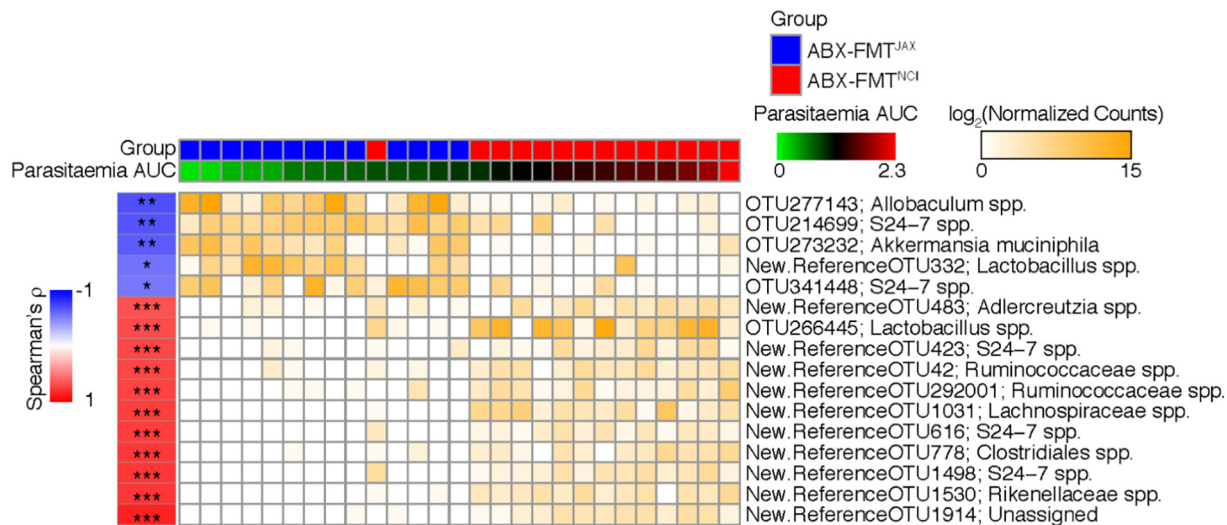


**Fig. 3.** Correlation between parasite burden and OTU abundance in ABX-FMT[NCI] and ABX-FMT[JAX] mice. Faecal pellets were collected from infected (Mal+) ABX-FMT[NCI] and ABX-FMT[JAX] mice between experimental days −10 to −1 for faecal microbiota analysis. The log2-transformed rarefied count values of OTUs that significantly correlate with parasite burden over the course of infection, represented by parasitaemia area under the curve (AUC), are depicted as a heat map (Spearman Correlation, FDR $q <$ *0·05; **$q \le 0.01$; *** $q \le 0.001$).

viability was observed between infected CTRL-FMT[JAX] mice (n = 5 dams, 57/69 or 83% viability) and infected CTRL-FMT[NCI] mice (n = 6 dams, 68/81 or 84% viability; P = 0·8300, two-tailed Fisher exact test), consistent with the similar parasite burdens observed in these animals (Supp. Fig. 7d). In addition, no significant difference in foetal viability was observed between uninfected CTRL-FMT[NCI] mice (n = 6 dams, 72/79 or 91% viability) and uninfected CTRL-FMT[JAX] mice (n = 6 dams, 67/71 or 94% viability; P = 0·5400, two-tailed Fisher exact test).

### 3.5. Maternal infection severity influences foetal weight at gestational term

Following the sacrifice of infected and uninfected dams at GD/ED 18, viable foetuses and placentae were weighed to assess the impact of maternal infection on foetal growth. Mixed linear models were utilized to assess the impact of infection severity, antibiotic treatment, and FMT group on foetal weights while accounting for the lack of independence between littermates. Parasite burden, represented by parasitaemia AUC value (Fig. 2d, Supp. Fig. 7d), antibiotic treatment status, and faecal microbiota transplant group account for 34·3% of the variance in foetal weight between dams (P < 0·001). With antibiotic treatment status and faecal microbiota transplant group held constant, each unit increase in parasitaemia AUC was found to be associated with a −0·0003 g reduction in the weight of each foetus on average (P = 0·0027). Summary data depicting foetal weights pooled by dam cohort for all groups of infected and uninfected antibiotic-treated (Supp. Fig. 9b) and antibiotic-free control dams (Supp. Fig. 10b) are presented for the purposes of visualization.

Maternal antibiotic treatment status also exerted a significant influence on foetal weight. Antibiotic treatment was found to be associated with a 0·1417 g increase in the weight of each foetus on average (P = 0·0009) when parasitaemia AUC value and FMT treatment group were held constant. However, this weight increase is neutralized if parasitaemia AUC is considered (interaction term, P = 0·0049; weight increase, 0·0002 g).

Placental weight was not significantly influenced by any of the variables included in analysis. For visualization, placental weight data are depicted in summary form, pooled by maternal infection status and treatment group (Supp. Fig. 9c, Supp. Fig. 10c). Foetal and placental weights are also shown by individual dams (Supp. Fig. 11) to demonstrate the variability within and between dams in a cohort.

### 3.6. Maternal infection severity influences neonatal survival in the first days of life, but surviving pups develop normally prior to weaning

To evaluate postnatal growth in the absence of variable maternal morbidity, pups produced by ABX-FMT[NCI] and ABX-FMT[JAX] donor dams were delivered by caesarean section and placed with unmanipulated NCI-sourced Swiss Webster foster dams with zero- to three-day-old litters. Fostering success and fostered pup survival at weaning are described in Table 1. Of the successfully mated females that met the weight gain threshold for pregnancy, pregnancy loss was only observed within the infected ABX-FMT[NCI] cohort (Table 1).

Although foster dams were not disturbed for three days following fostering to minimize stress-induced pup loss, foster pup attrition during this early postnatal period was substantial in all groups (Table 1). Survival to four days of age and weaning age did not differ significantly between the fostered progeny of uninfected ABX-FMT[NCI] dams and uninfected ABX-FMT[JAX] dams (Table 1). However, a significant reduction in fostered pup survival was observed in the progeny of infected ABX-FMT[NCI] dams compared to infected ABX-FMT[JAX] dams by day four (Table 1), suggesting that maternal infection severity is inversely related to early postnatal fitness.

When the fostered pups reached 4 days of age, they were individually identified by footpad tattooing and weighed every 3 days until weaning at 22 days of age. Trends in pup growth were analysed by linear mixed models. No significant relationships between maternal parasite burden or maternal treatment group and pup growth trends were detected, but the model did reveal that the number of total pups (native and fostered) in the litter at weaning significantly influenced the pup growth trajectory. Furthermore, the sex of the pup exerted an effect that varied over time (interaction term, P = 0·0277). Raw pup weights are depicted (Supp. Fig. 12) for the purposes of data visualization only. Although neither dam infection severity nor treatment group influenced trends in pup growth, pup weights are presented grouped by dam cohort for the purposes of illustration.

Pups were visually sexed at weaning. No significant difference in sex ratio was observed between infected dams (Supp. Table 2).

### 3.7. Peripheral cytokine levels are not significantly impacted by maternal infection severity or pregnancy

While dams receiving ABX-FMT[JAX] treatment and their progeny appear to be protected from the high parasite burdens and poor birth outcomes observed in highly susceptible ABX-FMT[NCI] dams, the mechanisms underlying this protective effect are unknown. To explore the immunological differences between cohorts that could explain these differences, the peripheral inflammatory environment around the time of peak infection in dams experiencing relatively high and relative low parasite burdens was explored. GD/ED 10 was particularly desirable for this analysis since it corresponds to a period of weight stasis in ABX-FMT[NCI] but not ABX-FMT[JAX] mice (Fig. 2c). Unlike the previously described experiments, unmanipulated NCI-sourced mice were used as malaria-susceptible comparators for the relatively resistant ABX-FMT[JAX] mice. NCI-sourced mice are a suitable proxy for ABX-FMT[NCI] mice as the development of *P. chabaudi chabaudi* AS infection is similar in these cohorts [Morffy Smith, in review]. Levels of IFN-γ, TNF-α, IL-1β, IL-6, and IL-17A, as well as IL-10, were analysed in the peripheral plasma of gravid and virgin Mal + NCI-sourced and ABX-FMT[JAX] mice at GD/ED 10 (Fig. 4). Notably, no significant differences in levels of any of the aforementioned cytokines were observed as a function of gut microbiota-mediated susceptibility to infection or pregnancy status.

**Table 1**
Fostering success and survivorship. A significant difference in the proportion of total pups suitable for fostering was observed between maternal treatment groups only between cohorts of infected mice (two-tailed Fisher exact test). Similarly, a significant difference in the proportion of fostered pups surviving to weaning was observed between maternal treatment groups only between cohorts of infected mice (two-tailed Fisher exact test).

| Group | Dams producing live foetuses/Total dams | P | No. resuscitated/Total neonates | P | Pup no. 4, 22 days of age | Weaned/Fostered pups | P |
|---|---|---|---|---|---|---|---|
| Uninfected ABX-FMT[NCI] | 8/8 | 1 | 82/96 (85%) | 0·6394 | 48, 47 | 47/81 (58%) | 0·4365 |
| Uninfected ABX-FMT[JAX] | 5/5 | | 42/51 (82%) | | 29, 28 | 28/42 (67%) | |
| Infected ABX-FMT[NCI] | 7/13 | 0·1093 | 28/61 (46%) | <**0·0001** | 10, 9 | 9/26 (35%) | **0·0014** |
| Infected ABX-FMT[JAX] | 6/6 | | 61/64 (95%) | | 45, 44 | 44/60 (73%) | |

Bold font indicates statistical significance.

### 3.8. Maternal malaria infection severity influences the uterine environment

Although differences in peripheral cytokine titres were not observed as a function of infection severity, the local immunological milieu within the uterus was investigated to determine if relatively high or low maternal parasite burdens altered the intrauterine environment around the time of peak infection. Malaria-exposed conceptuses and unexposed controls collected from NCI-sourced dams and ABX-FMT[JAX] dams at GD/ED 10 were subjected to gene expression analysis to assess local cytokine production as well as the abundance of monocytes, neutrophils, and natural killer (NK) cells. Monocytes were selected for investigation because monocyte infiltration, or intervillositis, is considered characteristic of gestational malaria infection in humans, and is positive associated with poor birth outcomes [11,12,15,58]. Neutrophils were selected because the accumulation of these cells has also been reported in *P. falciparum*-infected placentae [59]. Finally, NK cells were selected because these cells are a major cell subset in the uterus that play a critical role in normal placental development (reviewed by Faas and de Vos, 2017) [60].

Transcripts of cytokines including IFN-γ, TNF-α, IL-1β, and IL-10, and the chemokine MCP-1/CCL2, did not vary between groups in the absence of infection (Fig. 5a). In conceptuses collected from both groups of malaria-infected dams, the expression of *Ifng* was significantly elevated compared to uninfected treatment-matched controls. Among conceptuses collected from NCI-sourced dams, exposure to malaria infection was associated with a significant increase in *Il10* expression (Fig. 5a). Among ABX-FMT[JAX] conceptuses exposed to lower parasite burdens, infection was not associated with elevated *Il10* expression (Fig. 5a). No differences in *Tnf* and *Il1b* expression were observed in response to infection, regardless of disease severity (Fig. 5a).

*Mgl2*, *Ncf2*, and *Klrd1* are expressed by macrophages, neutrophils, and NK cells, respectively [61]. The relative abundance of these cell types was determined by assessing the transcript abundance of these genes. *Ncf2* and *Klrd1* expression was similar across groups (Fig. 5b). In contrast, *Mgl2* expression was elevated in malaria-infected dams relative to controls, though the enhancement reached statistical significance only in ABX-FMT[JAX] dams (Fig. 5b). Notably, three NCI-sourced dams exhibited exceptionally high *Mgl2* transcript levels (Fig. 5b). A few factors could result in the significant variance observed within the cohort. First, the malaria-exposed NCI-sourced conceptuses exhibiting the highest *Mgl2* expression had relatively high parasite burdens at the time of sacrifice (Fig. 5c), with parasitaemia being significantly
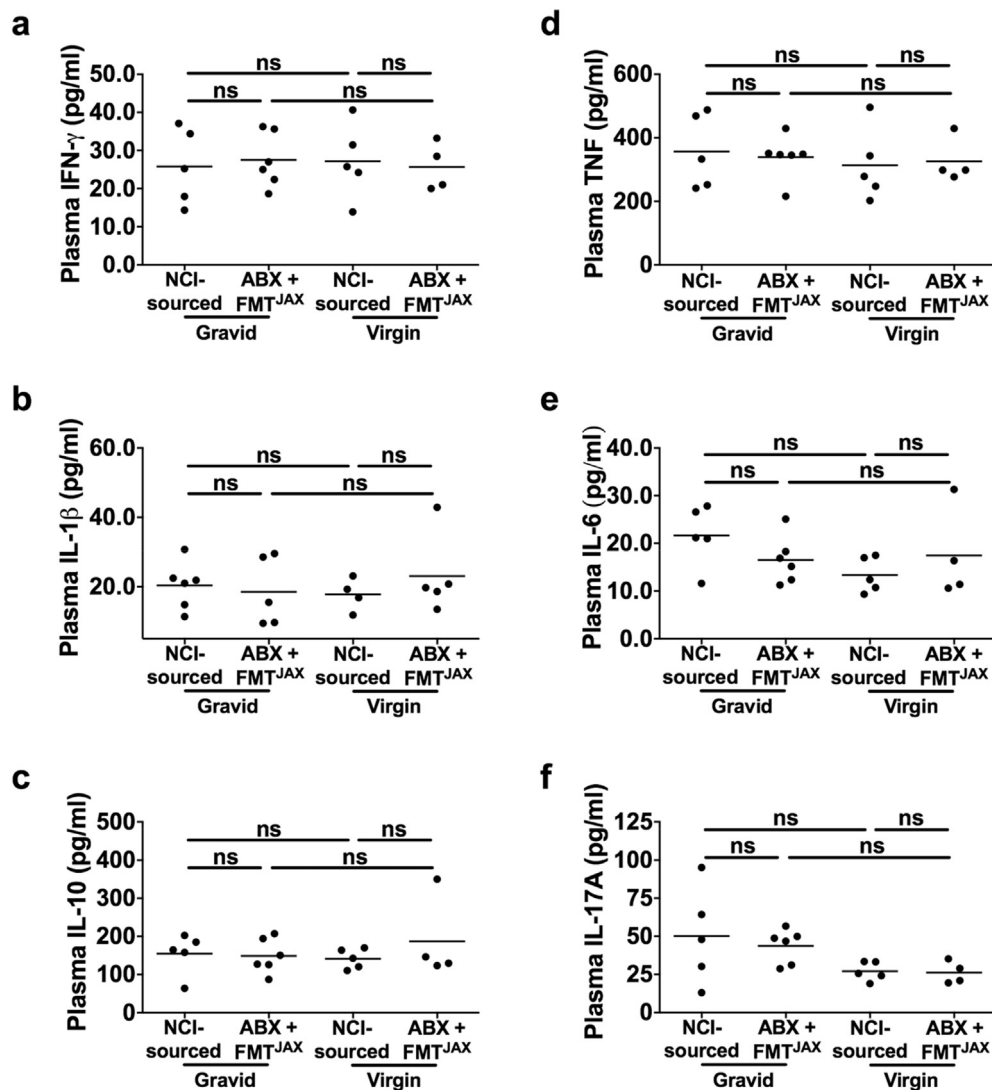


**Fig. 4.** Plasma cytokine titres in virgin and gravid *P. chabaudi chabaudi* AS-infected NCI-sourced and ABX-FMT[JAX] mice. No significant differences in cytokine titres measured in peripheral plasma were observed as a function of pregnancy status or treatment group in malaria-infected (Mal+) and uninfected (Mal-) gravid and virgin mice at GD/ED 10 ($P > 0.05$; Kruskal-Wallis test with Dunn's post-test for multiple comparisons). a. IFN-γ. b. IL-1β. c. IL-10. d. TNF. e. IL-6. f. IL-17A. Virgin Mal + ABX-FMT[JAX] $n = 4$; Gravid Mal + ABX-FMT[JAX] $n = 6$; Virgin Mal + NCI-sourced $n = 5$; Gravid Mal + NCI-sourced $n = 5$; ns $P > 0.05$.
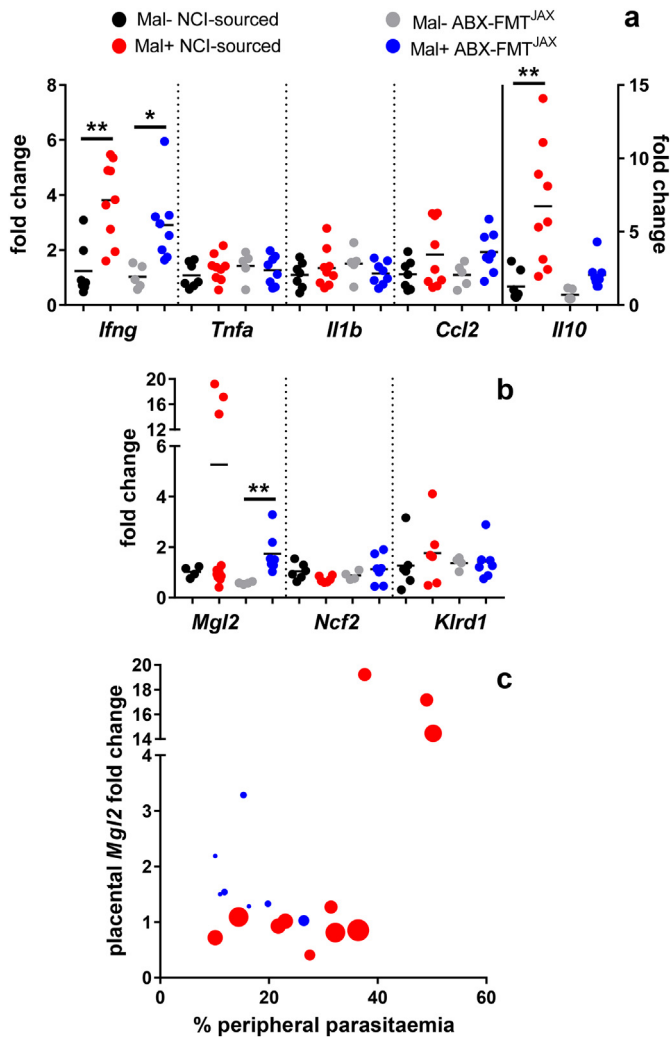
**Fig. 5.** Malaria-induced expression of cytokine, chemokine, and cell-type specific genes in *P. chabaudi chabaudi* AS-exposed conceptuses. Gene expression was evaluated in conceptuses collected from malaria-infected (Mal+) and uninfected (Mal-) dams sacrificed at GD/ED 10. a. Transcript levels of mouse *Ifng*, *Tnf*, *Il1b*, *Il10*, and *Ccl2* were quantified by qPCR. Transcript abundance in all samples was internally normalized to *Ubc*. Transcription in Gravid Mal + NCI-sourced, Gravid Mal- ABX-FMT^JAX, and Gravid Mal + ABX-FMT^JAX samples is presented relative to transcription in Gravid Mal- NCI-sourced samples. Statistically significant differences in the expression of *Ifng* are observed between malaria-infected (Mal+) and uninfected (Mal-) NCI-sourced mice (*P* = 0·0045) and ABX-FMT^JAX mice (*P* = 0·0397; Kruskal-Wallis test with Dunn's post-test for multiple comparisons). A statistically significant difference in the expression of *Il10* is observed between Mal + and Mal- NCI-sourced (*P* = 0·003; Kruskal-Wallis test with Dunn's post-test for multiple comparisons). Gravid Mal- NCI-sourced *n* = 7; Gravid Mal + NCI-sourced *n* = 9; Gravid Mal- ABX-FMT^JAX *n* = 5; Gravid Mal + ABX-FMT^JAX *n* = 8. b. Transcript levels of mouse *Mgl2*, *Ncf2*, and *Klrd1* were quantified by qPCR. Transcript abundance in all samples was internally normalized to *Gapdh*. Transcription in Gravid Mal + NCI-sourced, Gravid Mal- ABX-FMT^JAX, and Gravid Mal + ABX-FMT^JAX samples is presented relative to transcription in Gravid Mal- NCI-sourced samples. A statistically significant difference in the expression of *Mgl2* is observed between Mal + and Mal- NCI-sourced (*P* = .0027; Kruskal-Wallis test with post-test for multiple comparisons). *Mgl2*: Gravid Mal- NCI-sourced *n* = 4; Gravid Mal + NCI-sourced *n* = 11; Gravid Mal- ABX-FMT^JAX *n* = 4; Gravid Mal + ABX-FMT^JAX *n* = 7. *Ncf2* and *Klrd1*: Gravid Mal- NCI-sourced *n* = 6; Gravid Mal + NCI-sourced *n* = 6; Gravid Mal- ABX-FMT^JAX *n* = 4; Gravid Mal + ABX-FMT^JAX *n* = 7. c. Transcript abundance of *Mgl2*, presented as fold change, is presented as a function of peripheral parasitaemia at the time of sacrifice. Points, representing conceptuses collected from individual dams, are scaled according to parasitaemia AUC value, with larger points corresponding to higher parasite burdens over the course of the experiment (GD 0 to GD/ED 10). A statistically significant relationship between *Mgl2* fold change and parasitaemia at the time of sacrifice is observed by linear regression analysis (*P* = 0·001). Gravid Mal + NCI-sourced *n* = 11; Gravid Mal + ABX-FMT^JAX *n* = 7. * *P* < 0·05; ** *P* < 0·01.

associated with transcript levels (*P* < 0.001, by linear regression analysis). Second, these conceptuses were derived from dams whose parasitaemia had not yet peaked; those with lower *Mgl2* transcript levels had experienced peak infection on the previous day, suggesting that *Mgl2* expression may decline following the achievement of peak parasitaemia. Interestingly, *Mgl2* expression at this time point was independent of the overall parasite burden (AUC from GD/ED 0 to 10) experienced by the dams (Fig. 5c).

To visualize inflammatory cell abundance in the midgestational placentae, haematoxylin and eosin-stained thin sections of NCI-sourced and ABX-FMT^JAX conceptuses were examined microscopically. Two samples with comparable peripheral and placental parasitaemia are depicted to illustrate that inflammatory cell infiltrate in maternal blood sinusoids is enhanced in NCI-sourced relative to ABX-FMT^JAX mice (Fig. 6a, b). Remarkably, most of these cells in the former group contained phagocytosed haemozoin. To further characterize accumulation of haemozoin in malaria-infected placentae, micrographs were subjected to image analysis. Relative to ABX-FMT^JAX conceptuses, NCI-sourced placentae tended to bear higher haemozoin loads (Fig. 7a), consistent with the higher parasite burdens observed in these animals.

In addition to facilitating haemozoin enumeration, our analysis also revealed a significant reduction in maternal vascular space in malaria-infected NCI-sourced relative to malaria-infected ABX-FMT^JAX placentae (Fig. 7b). This finding was corroborated by direct tallies of prominent maternal blood sinuses in images of placental junctional zone in the two groups; whereas 143/446 (32·1%) micrographs of ABX-FMT^JAX placentae revealed maternal blood spaces, only 94/472 (19·9%) micrographs of NCI-sourced mice had similar evidence (*P* < 0·0001).

## 4. Discussion

Genetic traits exert significant influence on the susceptibility of mice to experimental malaria infection. Studies utilizing inbred mice reveal that some strains of congenic mice, including A/J and BALB/c, are relatively susceptible to *P. chabaudi chabaudi* AS infection, while C57BL/6 J and CBA mice are relatively resistant to malaria [62]. Strain-dependent differences in susceptibility persist in the context of pregnancy. Pregnant A/J mice are more susceptible to malaria infection than pregnant C57BL/6 J mice following infection in early gestation (GD 0), although both A/J and C57BL/6 mice uniformly abort their pregnancies at midgestation [31]. The production of recombinant inbred strains by crossing mice from different strains enabled the identification of genetic loci governing murine susceptibility to *P. chabaudi chabaudi* AS infection [62]. Strikingly, the present study finds that the composition of the gut microbiota informs malaria infection severity in a genetically diverse population of outbred Swiss Webster mice, indicating that genetic traits are not the only factors governing susceptibility to murine malaria infection.

We report that the composition of the gut microbiota supersedes genetic determinants of malaria infection severity and pregnancy outcome in an outbred mouse model for gestational malaria. Compared to Swiss Webster mice that received a susceptibility-conferring faecal microbiota transplant following antibiotic treatment (ABX-FMT^NCI), Swiss Webster mice that received a malaria resistance-conferring faecal microbiota transplant following antibiotic treatment (ABX-FMT^JAX) subsequently developed lower parasite burdens during pregnancy and were protected from malarial anaemia and infection-associated reductions in gestational weight gain. Furthermore, the reduction in parasite burden observed in ABX-FMT^JAX mice was associated with improved foetal and postnatal outcomes.

The larger maternal parasite burdens observed in ABX-FMT^NCI, CTRL-FMT^NCI, and CTRL-FMT^JAX mice compared to ABX-FMT^JAX dams had a modest negative impact on foetal weight at term. In contrast, maternal antibiotic treatment was associated with a relatively large increase in foetal weight at term, regardless of gut microbiota donor or parasite burden, though this effect was significant tempered by
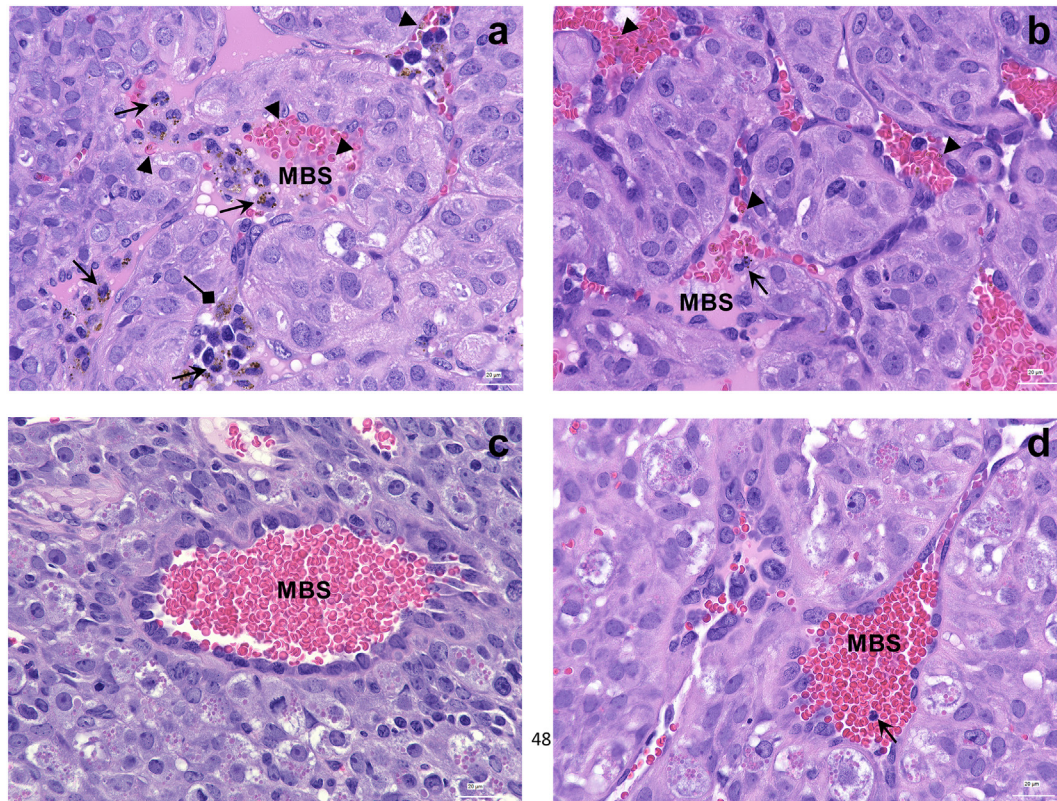
**Fig. 6.** Micrographs of malaria-infected placental sections at GD/ED 10. a. Placental junctional zone of an NCI-sourced dam with 23·0% peripheral and 31·6% placental parasitemia, showing maternal blood sinusoids (MBS) with numerous iRBCs (arrowheads) and maternal inflammatory cells, most containing phagocytosed haemozoin (arrows). Some haemozoin in trophoblasts is evident in this view (diamond arrows). b. Placental junctional zone of an ABX-FMT[JAX] dam with 25·9% peripheral and 29·3% placental parasitemia, showing a MBS with iRBCs (arrowheads) and infrequent maternal inflammatory cells containing phagocytosed haemozoin (arrows). c. Placental junctional zone of an uninfected NCI-sourced dam. No leukocytes are evident in the MBS in this view. d. Placental junctional zone of an uninfected ABX-FMT[JAX] dam showing a single leukocyte (arrow) in the MBS.

infection. The mechanism(s) by which maternal antibiotic treatment prior to pregnancy enhances foetal growth is unknown. Previous research in mice has demonstrated that maternal antibiotic treatment can promote adiposity in offspring after birth, although these studies entailed the peripartum antibiotic treatment of the dam [63,64]. In the experiments described here, dams completed the antibiotic treatment course approximately two weeks prior to mating and the initiation of infection. Furthermore, the impact of antibiotic treatment during lactation on postnatal growth was not assessed in this study, so it is not possible to directly compare the results presented here with previously published work.

Although foetal viability at GD 18, as determined by in situ reactive movement in the womb, was similar between the populations of foetuses produced by infected ABX-FMT[NCI] and infected ABX-FMT[JAX] dams, we found that fewer pups derived from the former could be resuscitated following caesarean delivery at this time point. Furthermore, we observed that postnatal survival was significantly reduced in the progeny of infected ABX-FMT[NCI] dams compared to their ABX-FMT[JAX] counterparts. These data suggest that foetal movement in the uterus at term is a poor predictor of neonatal fitness. As fostering was performed to control for the potential impact of abnormal maternal behaviour due to infection, neonatal mortality among the progeny of infected ABX-FMT[NCI] dams cannot be attributed to maternal illness. Instead, these data suggest that the progeny of infected ABX-FMT[NCI] dams are less fit at GD 18, albeit with only modest infection-associated reduction in foetal weight. The mechanisms by which high maternal parasite burdens reduce postnatal survival in the progeny of infected ABX-FMT[NCI] dams compared to the progeny of infected ABX-FMT[JAX] dams are unknown. We speculate that fostered pups produced by infected ABX-FMT[NCI] dams are less able to compete for limited maternal resources, especially in a litter that contains healthy native pups, but the specific

physiological changes that reduce fitness remain for future studies to explore.

The divergent infection trajectories reported in ABX-FMT[NCI] and ABX-FMT[JAX] mice were associated with distinct communities of gut microbes that were observed in these cohorts of mice within the days prior to parasite exposure. We cannot rule out persistence of some endogenous gut microbes in the ABX-treated mice, including those that might be resistant to the aggressive treatment regimen applied in this work. Post-antibiotic treatment differences between the gut microbiota in ABX-FMT[NCI] and ABX-FMT[JAX] mice may reflect vendor-dependent differences in the composition of the gut microbiota of the NCI-sourced and JAX-derived mice used as faecal donors. This phenomenon can be attributed to environmental factors, such as husbandry practices or diet, as well as the genetic traits of the murine population propagated at a given facility [65–67]. However, NCI-sourced Swiss Webster mice were used as faecal donors for mice receiving FMT[NCI] while JAX-derived C57BL/6 mice were used as faecal donors for mice receiving FMT[JAX]. Thus, differences in gut microbiota observed between ABX-FMT[NCI] and ABX-FMT[JAX] recipient mice may reflect mouse strain- or stock-specific, but not vendor-specific, differential microbial communities. The innate immunological differences between mouse strains may shape the composition of the gut microbiota, yielding mouse strain-specific variance among mice obtained from the same vendor [43]. Furthermore, gut-resident eukaryotic commensals can have immunomodulatory capabilities [68], and we cannot currently exclude the possibility that such eukaryotes contributed to the modulation of malaria infection severity in mice receiving faecal microbiota transplants from different donors.

The composition of the gut microbiota in antibiotic-treated faecal microbiota transplant recipient mice may not faithfully recapitulate the composition of the gut microbiota of donor mice. First, the bacteria
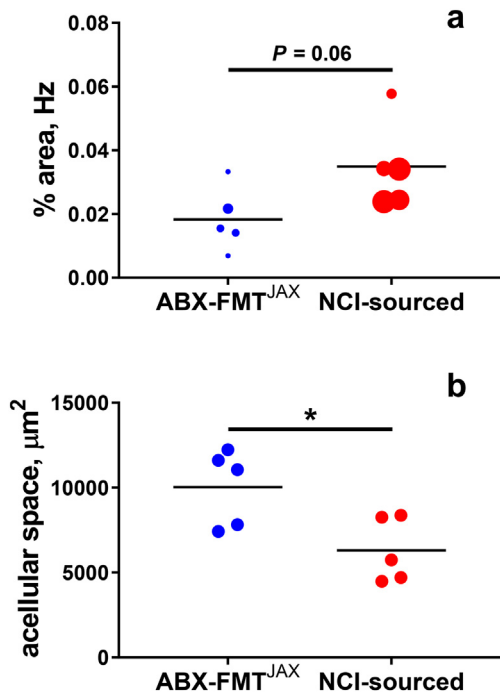
**Fig. 7.** Haemozoin quantification in the placentae of malaria-exposed conceptuses at midgestation. a. Haemozoin (Hz) density was measured by image analysis and is depicted as the percentage of haemozoin-occupied area in micrographs of the junctional zone. Points, depicting individual dams, are scaled according to parasitaemia AUC value (GD/ED 0 to GD/ED 10). A tendency for increased haemozoin abundance in NCI-sourced relative to ABX-FMT[JAX] placentae is evident ($P = 0.0599$; Student's $t$-test). Maternal vascular space in placental junctional zone estimated as a function of acellular areas identified by imaging software, corrected for total number of images examined. Vascular space is significantly reduced in NCI-sourced relative to ABX-FMT[JAX] placentae (*$P = 0.022$; Student's $t$-test).

administered by the oral gavage of faecal slurries may not closely resemble the communities of bacteria in the gut lumen, because the population of bacteria in the faeces differs from the population of microbes within the gut lumen [69,70]. In addition, our preparation of faecal slurries may further bias the composition of the administered bacterial communities. Faecal slurries were briefly centrifuged prior to administration for the removal of particulate matter too large to pass through the gavage needle. It is possible that this processing removed bacteria that were closely associated with this fibrous material. Furthermore, faecal samples were collected and faecal slurries prepared under normoxic conditions. Previous study of human faecal microbiota transplants has revealed that oxygen exposure can damage faecal microbial communities [71]. Such processing may also exclude anaerobes. For these reasons, we do not claim that the post-treatment faecal microbiota of antibiotic-treated, faecal microbiota transplanted mice closely resembles the faecal microbial communities of the donor groups, although we do demonstrate that antibiotic treatment followed by the administration of a faecal microbiota transplant consisting of faecal samples collected from JAX-lineage or NCI-sourced mice results in distinct communities of faecal microbes in recipients.

Host immunity exerts selective pressure on the gut microbiota, shaping the composition of this community [43]. Thus, we anticipate that host selection within FMT recipients may influence the gut microbial community prior to malaria infection. Host-driven selection may explain the discrepancy in microbial diversity observed between ABX-FMT[NCI] and ABX-FMT[JAX] recipients. Intriguingly, malaria-resistant ABX-FMT[JAX] mice displayed significantly reduced faecal microbial diversity compared to susceptible ABX-FMT[NCI] mice. This finding is inconsistent with previous studies demonstrating that reduced gut microbial diversity, representing dysbiosis, correlated with poor health outcomes associated with uncontrolled inflammation, resulting in preterm birth

[72] and metabolic disorders [73–75]. Furthermore, antibiotic-induced dysbiosis was associated with enhanced susceptibility to enteric [76] and systemic pathogens [77]. However, this result supports the hypothesis that host-driven selection may be induced in FMT recipients. Specifically, the contraction in community diversity observed in ABX-FMT[JAX] mice compared to ABX-FMT[NCI] mice may reflect the elimination of microbes in C57BL6-produced FMT[JAX] donor faeces from the lumen of the Swiss Webster gut. In contrast, the bacterial communities in Swiss Webster-produced FMT[NCI] faeces may experience similar selective pressures in both the donor and recipient Swiss Webster animals. Alternatively, the contraction in community diversity observed in ABX-FMT[JAX] mice compared to ABX-FMT[NCI] mice may reflect both the diversity of the donor faecal microbial communities and the competition with residual endogenous microbes.

In a recent study using unmanipulated inbred mice sourced from different vendors, an increased abundance of Clostridiaceae, Erysipelotrichaceae, Lactobacillaceae, and Peptostreptococcaceae family members was linked to lower parasite burdens following infection with multiple murine malaria species, while a greater abundance of Bacteroidaceae, Prevotellaceae, and Sutterellaceae family members was associated with susceptibility [38,39]. Consistent with this notion, we found that Erysipelotrichaceae family members were enriched in malaria-resistant ABX-FMT[JAX] mice compared to malaria-susceptible ABX-FMT[NCI] mice. However, contrary to the observations made in inbred animals, we observed enrichment of Lactobacillaceae in malaria-susceptible ABX-FMT[NCI] mice and an enrichment of Bacteroidaceae in malaria-resistant ABX-FMT[JAX] animals. There are numerous differences between our study and that previous elegant work that might explain such different outcomes. Most notably, previous studies describing the impact of gut microbiota on malaria infection utilized inbred mice. Perhaps some of the observed differences reflect inherent differences between inbred strains and outbred Swiss Webster mice.

A small proportion of OTUs were significantly negatively correlated with parasite burden. Among these, an OTU identified as a member of the genus *Allobaculum* and an OTU classified as *A. muciniphila* were unique because *Allobaculum* and *Akkermansia* species were significantly enriched in ABX-FMT[JAX] mice relative to ABX-FMT[NCI] mice. The remaining OTUs negatively associated with parasite burden were classified as S24-7 family members, which were not enriched in either group, and *Lactobacillus* species, which were actually enriched in ABX-FMT[NCI] mice. Notably, the enrichment of *Allobaculum* species has previously been observed in malaria-resistant C57BL/6 mice sourced from JAX [39]. The mechanism by which *Allobaculum* species might modify susceptibility to malaria has not yet been interrogated, but these bacteria have previously been identified as members of a healthy murine gut microbiota associated with protection against obesity and other inflammatory metabolic conditions [78]. The enrichment of *Akkermansia* species has not previously been observed in mice displaying microbiota-induced resistance to malaria infection, although *A. muciniphila* has previously been identified as an immunomodulatory component of the gut microbiota in mice and humans [79]. The abundance of *A. muciniphila* is negatively associated with obesity and related metabolic disorders in mice [78,80] and humans [81,82]. *A. muciniphila* may contribute to the prevention of these inflammatory disorders by promoting the integrity of the intestinal epithelial barrier [83,84]. Furthermore, the enrichment of *A. muciniphila* within gut microbiota of human patients receiving anti-PD-1-based immunotherapies for epithelial tumours is associated with improved survival [85]. In mice, combined treatment with PD-1 blockade therapies and *A. muciniphila* was associated with a protective anti-tumour Th1 response [85]. A robust Th1 response controls acute *P. chabaudi chabaudi* AS infection in inbred mice [86]; thus, *A. muciniphila* may fortify the Th1-biased antimalarial immune response in ABX-FMT[JAX] mice, promoting resistance to malaria infection. The extent to which the differences in malaria infection outcomes observed here are dependent on gut microbiota-influenced immune responses is an area that deserves further intensive study.

We did not examine the composition of the gut microbiota in either CTRL-FMT[NCI] or CTRL-FMT[JAX] mice. As these animals exhibited parasite burdens similar to those observed in ABX-FMT[NCI] mice, we speculate that the composition of the gut microbiota in CTRL-FMT[NCI] and CTRL-FMT[JAX] mice was not enriched in the OTUs associated with resistance to malaria infection in ABX-FMT[JAX] mice. Consistent with this, CTRL-FMT[NCI] and CTRL-FMT[JAX] mice developed high parasite burdens similar to those observed in ABX-FMT[NCI] animals. Previous studies have demonstrated that exogenous gut microbes do not efficiently engraft in the gut in the absence of a niche created by antibiotic pretreatment [39,87]. As expected, assessment of gut microbial content from two time points spanning the antibiotic regimen applied to ABX mice, which was not applied to CTRL mice, showed no change in gut bacterial load in the latter. Thus, we posit that the composition of the gut microbiota in the CTRL-FMT groups closely resembles the gut microbiota of unmanipulated NCI-sourced Swiss Webster mice or the gut microbiota of ABX-FMT[NCI] mice, as these animals were reconstituted with endogenous microbes.

Although this study exclusively probes the relationship between the composition of the gut microbiota prior to infection and malaria infection severity, it is important to note that malaria infection itself can influence the gut microbiota. In B6 and BALB/c mice, *P. berghei* ANKA infection is associated with intestinal pathology and the dysbiosis of the gut microbiota. Both intestinal pathology and dysbiosis were more profound in B6 mice, which are considered more susceptible to severe *P. berghei* ANKA infection [88]. Although the precise cause of this intestinal dysbiosis was not determined, dysbiosis in BALB/c mice with little to no intestinal pathology suggests that malaria infection or the immune response to malaria infection, not malaria-associated intestinal pathology, disrupts the gut microbiota [88]. Consistent with this, B6 mice infected with *P. yoelli* also display dysbiosis during infection, which recedes as the infection is cleared [89]. Moreover, mouse source/gut microbiota-specific differences in malaria susceptibility persist even after infection in this model is resolved; transfaunation of germ-free mice with faeces from previously infected mice exhibit the same susceptibility patterns as the original animals [90]. Although malaria-induced dysbiosis is transient, it can have significant functional consequences. For example, *P. yoelli*-infected B6 mice display reduced colonization resistance to non-typhoidal *Salmonella enterica* serotype Typhimurium [89]. Intriguingly, taxa we identify as associated with relative resistance or susceptibility to malaria infection are not consistently correlated with high or low parasite burdens in mice experiencing malaria-associated dysbiosis. These discrepancies may again be attributable to differences in parasite and mouse strains. However, as the present study does not evaluate changes to the gut microbiota over the course of the experiment, these studies cannot be directly compared. The modulation of ongoing malaria infection severity by malaria-induced gut microbiota dysbiosis in outbred mice remains to be investigated. Interesting clues from the B6/*P. yoelli* system are emerging, and indicate profound impacts on liver function, intestinal inflammation and gut microbial metabolism and functional capacity that vary as a function of vendor-specific microbial communities and the differential susceptibility to malaria that they confer [39,90].

The mechanisms by which some vendor-associated gut microbiota may reduce susceptibility to murine malaria infection are not understood. Previous work has attributed this difference to an accelerated T follicular helper cell response in mice colonized with malaria resistance-associated microbes, although the microbial products or bacterial gene products that drive this acceleration have not been identified [39]. Cross-reactive antibodies directed against specific microbes present in JAX-associated faeces and absent in NCI-associated faeces might be sufficient to neutralize blood-stage malaria parasites as was recently observed in mice colonized with *Escherichia coli* O86:B7, an isolate that expresses Galα1-3Galβ1-4GlcNAc-R (α-gal). The antibodies produced in response to *E. coli* O86:B7 targeted malaria sporozoites, which also bear α-gal on their surface, and protected mice against transmission

[91]. Finally, it is possible that microbial metabolites could also influence the immune response to infection or alter parasite growth, as recently demonstrated by the impairment of *Salmonella* growth by the *Bacteroides* product propionate [92]. However, recent work in inbred B6 mice suggests that faecal short-chain fatty acids, though variable across mice obtained from different vendors, cannot explain differential susceptibility to *P. yoelli* infection [93].

We hypothesized that the differences in susceptibility to malaria infection observed between ABX-FMT[NCI] and ABX-FMT[JAX] dams were attributable to gut microbiota-mediated differences in the immune response to infection. To investigate the immunological milieu in mice that were highly susceptible and relatively resistant to malaria infection, cohorts of NCI-sourced and ABX-FMT[JAX] mice were at sacrificed at GD/ED 10, around the time of peak infection, when stasis in weight gain in ABX-FMT[NCI] occurs. NCI-sourced mice were used as proxies for ABX-FMT[NCI] mice in these experiments, as NCI-sourced and ABX-FMT[NCI] mice experience a similar course of infection and comparable pregnancy outcomes [*Morffy Smith, in review*]. Peripheral cytokine levels were analysed to assess the systemic response to infection, and gene expression in malaria-exposed conceptuses was measured to explore the intrauterine environment. While the peripheral cytokine response was not influenced by infection severity at GD/ED 10, differences in the transcriptional response to infection were observed between malaria-exposed conceptuses. Though both groups of infected dams revealed elevated conceptus expression of *Ifng*, the expression of *Il10* was significantly greater in malaria-exposed conceptuses collected from NCI-sourced dams, but not in ABX-FMT[JAX] conceptuses, relative to uninfected controls. Consistent with this, IL-10 has been suggested as a biomarker of pathogenic, uncontrolled inflammation in human PM [94,95]. Transcription of *Mgl2* was also elevated in infected dams of both groups, but in NCI-sourced dams dramatic upregulation was observed only in those with the highest parasitaemias at the time of sacrifice. Thus, *Mgl2* levels were variable within the malaria-infected NCI-sourced cohort, perhaps reflecting differences in parasite dynamics or unique genetic characteristics of the individual animals. In this regard, it is also important to note that women with gestational malaria do not universally exhibit intervillositis [96]. As in an outbred human population, this discrepancy may reflect inherent differences in a genetically diverse population.

Accumulation of haemozoin in the *P. falciparum*-infected human placenta is a key feature of the infection, and, embedded in fibrin or present in infiltrating maternal phagocytes, is linked with pathogenesis [96]. Haemozoin accumulation in the infected Swiss Webster placenta is associated with enhanced anti-oxidant gene expression [*Morffy Smith, in review*] and may be a key driver of embryotoxic oxidative stress [49]. Compared to mid-gestational conceptuses from infected ABX-FMT[JAX] mice, infected NCI-sourced placentae tended to accumulate more haemozoin, with significant accumulation in both foetal (trophoblast) [*Morffy Smith, in review*] and maternal inflammatory cells. The extent to which the accumulated haemozoin directly contributes to pathogenesis is unclear, but it is noteworthy that the same group also had reduced maternal vascular spaces in imaged placentae. A similar observation was made in *P. berghei*-infected BALB/c mice [97]. Thus, reduced birthweight in term foetuses born to infected ABX-FMT[NCI] mice may be linked to reduced placental blood perfusion secondary to malaria-induced vascular disruption [98].

While evidence for the importance of the gut microbiota in determining malaria severity is accumulating in mouse models, the extent to which the composition of the gut microbiota may influence human susceptibility to malaria infection has not been extensively explored. At this time, few studies explore the relationship between the composition of the gut microbiota and malaria infection in humans. A study of children in Mali found that the gut microbiota composition was significantly associated with the risk of malaria infection, but was not significantly associated with the risk of developing febrile malaria following transmission [99]. Despite the dearth of evidence directly linking the

human gut microbiota to susceptibility to malaria infection, other studies hint at possible ties between the microbes within the gut and malaria. First, malaria infection in young children has long been recognized as a risk factor for invasive *Salmonella* infection [100], an effect that may be due to the immune response to malaria infection [101] and dysbiosis of the gut microbiota resulting from malaria infection [89]. However, in contrast to observations made in mice [88,89], a recent study conducted in Kenya found that *P. falciparum* infection and artemether-lumefantrine treatment did not significantly alter the composition of the gut microbiota in infants [102]. Thus, malaria-associated dysbiosis has yet to be directly linked to malaria infection in humans. Second, anti-α-gal antibodies have been identified as a component of the adaptive immune response against *P. falciparum* sporozoites in humans [91,103]. Although these antibodies are likely raised in response to sporozoites, it is possible that the ability of gut-resident *E. coli* species to produce α-gal could be exploited to protect people from transmission via a specifically designed probiotic cocktail intended to raise cross-reactive anti-α-gal antibodies, as previously described in mice [91].

While the identification of specific bacterial families or genera associated with relative resistance to malaria infection in humans is tantalizing, relationships between members of specific microbial communities and susceptibility to malaria remain challenging to pinpoint due to variable microbial diversity between individuals. In addition, identification of malaria resistance-associated microbial members in pregnant women will be further complicated by the changes observed in the human gut microbiota over the course of pregnancy [104]. Despite these challenges, the ability to alter susceptibility to malaria infection in the context of pregnancy as described herein provides at minimum a platform for the exploration of the relationship between maternal infection burden and foetal or postnatal outcomes. We have demonstrated that both malaria infection severity and pregnancy outcome can by influenced by modulating the composition of the gut microbiota in an outbred mouse model for malaria in pregnancy. This may facilitate the elucidation of malaria pathogenesis in the context of a high and a moderate density infection utilizing the same parasite-mouse combination.

The unique model presented here is further amenable to the exploration of mechanisms by which the gut microbes shape susceptibility to a systemic infection in the context of a genetically diverse population. Continued studies promise to yield new insights into the modulation of human responses to infection(s) by the functional microbial communities within the gut. Such research is warranted given rapidly accumulating evidence that the human gut microbiome significantly impacts local and systemic homeostasis and response to disease [105], including naturally elicited and vaccine-induced immune responses [106,107]. Advancing understanding of how the gut microbiome can be influenced through the use of prebiotics, probiotics, and selective antibiotics and other drugs provides potential mechanisms for supporting healthy or "protective" gut communities [108]. Overwhelmingly positive clinical results for control of *Clostridium difficile* infections through manipulation of the gut microbiome [109,110] have now opened the door for translating what we learn in animal model research, such as that reported here, and in myriad studies of disease associations with specific members of the gut microbial community, to clinical interventions. For malaria, in particular, for which decades of vaccine development and testing have yet to yield a licensed product [111], novel means of enhancing vaccine-induced immunity might include manipulation of the gut microbiome to include species associated with protection against malaria, an approach already receiving significant attention for infant vaccinations [106]. Given the importance of the maternal microbiome in shaping the pre- and post-natal gut microbial community [112,113], efforts to provide additional insights into microbiome complexity and how pathogens such as malaria may impact its dynamics should be high research priorities for these most vulnerable populations [114]. Prevention of poor pregnancy outcomes in patients infected

with malaria requires advanced, novel therapeutic approaches; accumulating evidence underscores the relevance of the gut microbiota and compels consideration of its potential modification during and after pregnancy as an emergent intervention.

## Funding sources

## Declaration of interests

The authors declare no competing interests.

## Author contributions

CDMS and JMM conceived and designed the experiments.
CDMS, CAC, and AKA contributed to the treatment, infection, and monitoring of mice, as well as data and sample collection throughout the experiments.
BNR performed image capture and haemozoin quantification.
CDMS performed descriptive statistical analyses and JMM performed mixed linear model analyses.
MG, MZ, YG and MM performed microbiota analysis and interpreted obtained data.
CDMS and JMM wrote the manuscript.

## Acknowledgments

## Appendix A. Supplementary data

Supplementary data to this article can be found online at https://doi.org/10.1016/j.ebiom.2019.05.052.

## References

[1] Rogerson SJ, Desai M, Mayor A, Sicuri E, Taylor SM, van Eijk AM. Burden, pathology, and costs of malaria in pregnancy: new developments for an old problem. Lancet Infect Dis 2018;18(4) [e107-e18].

[2] Walker PG, ter Kuile FO, Garske T, Menendez C, Ghani AC. Estimated risk of placental infection and low birthweight attributable to Plasmodium falciparum malaria in Africa in 2010: a modelling study. Lancet Glob Health 2014;2(8):e460–7.

[3] Bulmer JN, Rasheed FN, Morrison L, Francis N, Greenwood BM. Placental malaria. II. A semi-quantitative investigation of the pathological features. Histopathology 1993;22(3):219–25.

[4] Avery JW, Smith GM, Owino SO, et al. Maternal malaria induces a procoagulant and antifibrinolytic state that is embryotoxic but responsive to anticoagulant therapy. PLoS One 2012;7(2):e31090.

[5] Fried M, Duffy PE. Adherence of Plasmodium falciparum to chondroitin sulfate A in the human placenta. Science 1996;272(5267):1502–4.

[6] Khattab A, Kun J, Deloron P, Kremsner PG, Klinkert MQ. Variants of plasmodium falciparum erythrocyte membrane protein 1 expressed by different placental parasites are closely related and adhere to chondroitin sulfate A. J Infect Dis 2001; 183(7):1165–9.

[7] Muthusamy A, Achur RN, Bhavanandan VP, Fouda GG, Taylor DW, Gowda DC. Plasmodium falciparum-infected erythrocytes adhere both in the intervillous space and on the villous surface of human placenta by binding to the low-sulfated chondroitin sulfate proteoglycan receptor. Am J Pathol 2004;164(6):2013–25.

[8] Reeder JC, Cowman AF, Davern KM, et al. The adhesion of Plasmodium falciparum-infected erythrocytes to chondroitin sulfate A is mediated by P. falciparum erythrocyte membrane protein 1. Proc Natl Acad Sci U S A 1999;96(9):5198–202.

[9] Salanti A, Staalsoe T, Lavstsen T, et al. Selective upregulation of a single distinctly structured var gene in chondroitin sulphate A-adhering Plasmodium falciparum involved in pregnancy-associated malaria. Mol Microbiol 2003;49(1):179–91.

[10] Dorman EK, Shulman CE, Kingdom J, et al. Impaired uteroplacental blood flow in pregnancies complicated by falciparum malaria. Ultrasound Obstet Gynecol 2002; 19(2):165–70.

[11] Boeuf P, Aitken EH, Chandrasiri U, et al. Plasmodium falciparum malaria elicits inflammatory responses that dysregulate placental amino acid transport. PLoS Pathog 2013;9(2):e1003153.

[12] Dimasuay KG, Aitken EH, Rosario F, et al. Inhibition of placental mTOR signaling provides a link between placental malaria and reduced birthweight. BMC Med 2017;15(1):1.

[13] Chandrasiri UP, Chua CL, Umbers AJ, et al. Insight into the pathogenesis of fetal growth restriction in placental malaria: decreased placental glucose transporter isoform 1 expression. J Infect Dis 2014;209(10):1663–7.

[14] Umbers AJ, Boeuf P, Clapham C, et al. Placental malaria-associated inflammation disturbs the insulin-like growth factor axis of fetal growth regulation. J Infect Dis 2011;203(4):561–9.

[15] Dimasuay KG, Gong L, Rosario F, et al. Impaired placental autophagy in placental malaria. PLoS One 2017;12(11):e0187291.

[16] Cot M, Le Hesran JY, Miailhes P, Esveld M, Etya'ale D, Breart G. Increase of birth weight following chloroquine chemoprophylaxis during the first pregnancy: results of a randomized trial in Cameroon. Am J Trop Med Hyg 1995;53(6):581–5.

[17] Guyatt HL, Snow RW. Malaria in pregnancy as an indirect cause of infant mortality in sub-Saharan Africa. Trans R Soc Trop Med Hyg 2001;95(6):569–76.

[18] Luxemburger C, McGready R, Kham A, et al. Effects of malaria during pregnancy on infant mortality in an area of low malaria transmission. Am J Epidemiol 2001;154 (5):459–65.

[19] Steketee RW, Nahlen BL, Parise ME, Menendez C. The burden of malaria in pregnancy in malaria-endemic areas. Am J Trop Med Hyg 2001;64(1–2):28–35 Suppl.

[20] Steketee RW, Wirima JJ, Hightower AW, Slutsker L, Heymann DL, Breman JG. The effect of malaria and malaria prevention in pregnancy on offspring birthweight, prematurity, and intrauterine growth retardation in rural Malawi. Am J Trop Med Hyg 1996;55(1 Suppl):33–41.

[21] van Geertruyden JP, Thomas F, Erhart A, D'Alessandro U. The contribution of malaria in pregnancy to perinatal mortality. Am J Trop Med Hyg 2004;71(2 Suppl): 35–40.

[22] Murphy SC, Breman JG. Gaps in the childhood malaria burden in Africa: cerebral malaria, neurological sequelae, anemia, respiratory distress, hypoglycemia, and complications of pregnancy. Am J Trop Med Hyg 2001;64(1–2):57–67 Suppl.

[23] Le Port A, Watier L, Cottrell G, et al. Infections in infants during the first 12 months of life: role of placental malaria and environmental factors. PLoS One 2011;6(11): e27516.

[24] Tassi Yunga S, Fouda GG, Sama G, Ngu JB, Leke RGF, Taylor DW. Increased susceptibility to plasmodium falciparum in infants is associated with low, not high, placental malaria parasitemia. Sci Rep 2018;8(1):169.

[25] Natama HM, Rovira-Vallbona E, Sorgho H, et al. Additional screening and treatment of malaria during pregnancy provides further protection against Malaria and nonmalarial fevers during the first year of life. J Infect Dis 2018 May 25;217(12): 1967–76. https://doi.org/10.1093/infdis/jiy140.

[26] Hioki A, Hioki Y, Ohtomo H. Influence of pregnancy on the course of malaria in mice infected with Plasmodium berghei. J Protozool 1990;37(3):163–7.

[27] Oduola AM, Holbrook TW, Galbraith RM, Bank H, Spicer SS. Effects of malaria (Plasmodium berghei) on the maternal-fetal relationship in mice. J Protozool 1982;29 (1):77–81.

[28] Poovassery J, Moore JM. Murine malaria infection induces fetal loss associated with accumulation of Plasmodium chabaudi AS-infected erythrocytes in the placenta. Infect Immun 2006;74(5):2839–48.

[29] Poovassery J, Moore JM. Association of malaria-induced murine pregnancy failure with robust peripheral and placental cytokine responses. Infect Immun 2009;77 (11):4998–5006.

[30] Poovassery JS, Sarr D, Smith G, Nagy T, Moore JM. Malaria-induced murine pregnancy failure: distinct roles for IFN-gamma and TNF. J Immunol 2009;183(8): 5342–9.

[31] Sarr D, Bracken TC, Owino SO, et al. Differential roles of inflammation and apoptosis in initiation of mid-gestational abortion in malaria-infected C57BL/6 and A/J mice. Placenta 2015 Jul;36(7):738–49. https://doi.org/10.1016/j.placenta.2015.04.007 (Epub 2015 Apr 28).

[32] van Zon AA, Eling WM. Depressed malarial immunity in pregnant mice. Infect Immun 1980;28(2):630–2.

[33] Desai M, Ter Kuile FO, Nosten F, et al. Epidemiology and burden of malaria in pregnancy. Lancet Infect Dis 2007;7(2):93–104.

[34] Dellicour S, Tatem AJ, Guerra CA, Snow RW, ter Kuile FO. Quantifying the number of pregnancies at risk of malaria in 2007: a demographic study. PLoS Med 2010;7(1): e1000221.

[35] McGregor IA, Wilson ME, Billewicz WZ. Malaria infection of the placenta in the Gambia, West Africa; its incidence and relationship to stillbirth, birthweight and placental weight. Trans R Soc Trop Med Hyg 1983;77(2):232–44.

[36] Leke RF, Bioga JD, Zhou J, et al. Longitudinal studies of plasmodium falciparum malaria in pregnant women living in a rural Cameroonian village with high perennial transmission. Am J Trop Med Hyg 2010;83(5):996–1004.

[37] Watson-Jones D, Weiss HA, Changalucha JM, et al. Adverse birth outcomes in United Republic of Tanzania—impact and prevention of maternal risk factors. Bull World Health Organ 2007;85(1):9–18.

[38] Stough JM, Dearth SP, Denny JE, et al. Functional characteristics of the gut microbiome in C57BL/6 mice differentially susceptible to plasmodium yoelii. Front Microbiol 2016;7:1520.

[39] Villarino NF, LeCleir GR, Denny JE, et al. Composition of the gut microbiota modulates the severity of malaria. Proc Natl Acad Sci U S A 2016;113(8): 2235–40.

[40] Bracken TC, Cooper CA, Ali Z, Truong H, Moore JM. Helicobacter infection significantly alters pregnancy success in laboratory mice. J Am Assoc Lab Anim Sci 2017;56(3):322–9.

[41] Rakoff-Nahoum S, Paglino J, Eslami-Varzaneh F, Edberg S, Medzhitov R. Recognition of commensal microflora by toll-like receptors is required for intestinal homeostasis. Cell 2004;118(2):229–41.

[42] Reikvam DH, Erofeev A, Sandvik A, et al. Depletion of murine intestinal microbiota: effects on gut mucosa and epithelial gene expression. PLoS One 2011;6(3):e17996.

[43] Fransen F, Zagato E, Mazzini E, et al. BALB/c and C57BL/6 mice differ in polyreactive IgA abundance, which impacts the generation of antigen-specific IgA and microbiota diversity. Immunity 2015;43(3):527–40.

[44] Rodriguez-Palacios A, Aladyshkina N, Ezeji JC, et al. Cyclical Bias' in microbiome research revealed by a portable germ-free housing system using nested isolation. Sci Rep 2018;8(1):3801.

[45] Lightfoot YL, Yang T, Sahay B, et al. Colonic immune suppression, barrier dysfunction, and dysbiosis by gastrointestinal bacillus anthracis infection. PLoS One 2014;9(6):e100532.

[46] Colliou N, Ge Y, Sahay B, et al. Commensal Propionibacterium strain UF1 mitigates intestinal inflammation via Th17 cell regulation. J Clin Invest 2017;127(11): 3970–86.

[47] Caporaso JG, Kuczynski J, Stombaugh J, et al. QIIME allows analysis of high-throughput community sequencing data. Nat Methods 2010;7(5):335–6.

[48] Segata N, Izard J, Waldron L, et al. Metagenomic biomarker discovery and explanation. Genome Biol 2011;12(6):R60.

[49] Sarr D, Cooper CA, Bracken TC, Martinez-Uribe O, Nagy T, Moore JM. Oxidative stress: a potential therapeutic target in placental malaria. Immunohorizons 2017; 1(4):29–41.

[50] Sarr D, Smith GM, Poovassery JS, Nagy T, Moore JM. Plasmodium chabaudi AS induces pregnancy loss in association with systemic pro-inflammatory immune responses in A/J and C57BL/6 mice. Parasite Immunol 2012;34(4):224–35.

[51] Jimenez-Diaz MB, Mulet T, Gomez V, et al. Quantitative measurement of plasmodium-infected erythrocytes in murine models of malaria by flow cytometry using bidimensional assessment of SYTO-16 fluorescence. Cytometry A 2009;75 (3):225–35.

[52] Abatan OI, Welch KB, Nemzek JA. Evaluation of saphenous venipuncture and modified tail-clip blood collection in mice. J Am Assoc Lab Anim Sci 2008;47(3):8–15.

[53] Iwaki S, Matsuo A, Kast A. Identification of newborn rats by tattooing. Lab Anim 1989;23(4):361–4.

[54] Kulandavelu S, Qu D, Sunn N, et al. Embryonic and neonatal phenotyping of genetically engineered mice. ILAR J 2006;47(2):103–17.

[55] Adeghe AJ, Cohen J. A better method for terminal bleeding of mice. Lab Anim 1986; 20(1):70–2.

[56] Canobbio I, Visconte C, Momi S, et al. Platelet amyloid precursor protein is a modulator of venous thromboembolism in mice. Blood 2017;130(4):527–36.

[57] Schmittgen TD, Livak KJ. Analyzing real-time PCR data by the comparative C (T) method. Nat Protoc 2008;3(6):1101–8.

[58] Ordi J, Ismail MR, Ventura PJ, et al. Massive chronic intervillositis of the placenta associated with malaria infection. Am J Surg Pathol 1998;22(8):1006–11.

[59] Bostrom S, Schmiegelow C, Abu Abed U, et al. Neutrophil alterations in pregnancy-associated malaria and induction of neutrophil chemotaxis by Plasmodium falciparum. Parasite Immunol 2017;39(6).

[60] Faas MM, de Vos P. Uterine NK cells and macrophages in pregnancy. Placenta 2017; 56:44–52.

[61] Epiphanio S, Mikolajczak SA, Goncalves LA, et al. Heme oxygenase-1 is an anti-inflammatory host factor that promotes murine plasmodium liver infection. Cell Host Microbe 2008;3(5):331–8.

[62] Fortin A, Stevenson MM, Gros P. Complex genetic control of susceptibility to malaria in mice. Genes Immun 2002;3(4):177–86.

[63] Cho I, Yamanishi S, Cox L, et al. Antibiotics in early life alter the murine colonic microbiome and adiposity. Nature 2012;488(7413):621–6.

[64] Cox LM, Yamanishi S, Sohn J, et al. Altering the intestinal microbiota during a critical developmental window has lasting metabolic consequences. Cell 2014;158(4): 705–21.

[65] Ericsson AC, Davis JW, Spollen W, et al. Effects of vendor and genetic background on the composition of the fecal microbiota of inbred mice. PLoS One 2015;10(2): e0116704.

[66] Rausch P, Basic M, Batra A, et al. Analysis of factors contributing to variation in the C57BL/6J fecal microbiota across German animal facilities. Int J Med Microbiol 2016;306(5):343–55.

[67] Hufeldt MR, Nielsen DS, Vogensen FK, Midtvedt T, Hansen AK. Variation in the gut microbiota of laboratory mice is related to both genetic and environmental factors. Comp Med 2010;60(5):336–47.

[68] Chudnovskiy A, Mortha A, Kana V, et al. Host-protozoan interactions protect from mucosal infections through activation of the inflammasome. Cell 2016;167(2): 444–56 e14.

[69] Gu S, Chen D, Zhang JN, et al. Bacterial community mapping of the mouse gastrointestinal tract. PLoS One 2013;8(10):e74957.

[70] Pang W, Vogensen FK, Nielsen DS, Hansen AK. Faecal and caecal microbiota profiles of mice do not cluster in the same way. Lab Anim 2012;46(3):231–6.

[71] Chu ND, Smith MB, Perrotta AR, Kassam Z, Alm EJ. Profiling living bacteria informs preparation of fecal microbiota transplantations. PLoS One 2017;12(1):e0170922.

[72] Dahl C, Stanislawski M, Iszatt N, et al. Gut microbiome of mothers delivering prematurely shows reduced diversity and lower relative abundance of Bifidobacterium and streptococcus. PLoS One 2017;12(10):e0184336.

[73] Turnbaugh PJ, Hamady M, Yatsunenko T, et al. A core gut microbiome in obese and lean twins. Nature 2009;457(7228):480–4.

[74] Manichanh C, Rigottier-Gois L, Bonnaud E, et al. Reduced diversity of faecal microbiota in Crohn's disease revealed by a metagenomic approach. Gut 2006;55(2): 205–11.

[75] Menni C, Jackson MA, Pallister T, Steves CJ, Spector TD, Valdes AM. Gut microbiome diversity and high-fibre intake are related to lower long-term weight gain. Int J Obes (Lond) 2017;41(7):1099–105.

[76] Sekirov I, Tam NM, Jogova M, et al. Antibiotic-induced perturbations of the intestinal microbiota alter host susceptibility to enteric infection. Infect Immun 2008;76 (10):4726–36.

[77] Abt MC, Osborne LC, Monticelli LA, et al. Commensal bacteria calibrate the activation threshold of innate antiviral immunity. Immunity 2012;37(1):158–70.

[78] Everard A, Lazarevic V, Gaia N, et al. Microbiome of prebiotic-treated mice reveals novel targets involved in host response during obesity. ISME J 2014;8(10): 2116–30.

[79] Naito Y, Uchiyama K, Takagi T. A next-generation beneficial microbe: Akkermansia muciniphila. J Clin Biochem Nutr 2018;63(1):33–5.

[80] Everard A, Belzer C, Geurts L, et al. Cross-talk between Akkermansia muciniphila and intestinal epithelium controls diet-induced obesity. Proc Natl Acad Sci U S A 2013;110(22):9066–71.

[81] Zhang H, DiBaise JK, Zuccolo A, et al. Human gut microbiota in obesity and after gastric bypass. Proc Natl Acad Sci U S A 2009;106(7):2365–70.

[82] Santacruz A, Collado MC, Garcia-Valdes L, et al. Gut microbiota composition is associated with body weight, weight gain and biochemical parameters in pregnant women. Br J Nutr 2010;104(1):83–92.

[83] Chelakkot C, Choi Y, Kim DK, et al. Akkermansia muciniphila-derived extracellular vesicles influence gut permeability through the regulation of tight junctions. Exp Mol Med 2018;50(2):e450.

[84] Reunanen J, Kainulainen V, Huuskonen L, et al. Akkermansia muciniphila adheres to enterocytes and strengthens the integrity of the epithelial cell layer. Appl Environ Microbiol 2015;81(11):3655–62.

[85] Routy B, Le Chatelier E, Derosa L, et al. Gut microbiome influences efficacy of PD-1-based immunotherapy against epithelial tumors. Science 2018;359(6371):91–7.

[86] Su Z, Stevenson MM. Central role of endogenous gamma interferon in protective immunity against blood-stage plasmodium chabaudi AS infection. Infect Immun 2000;68(8):4399–406.

[87] Ji SK, Yan H, Jiang T, et al. Preparing the gut with antibiotics enhances gut microbiota reprogramming efficiency by promoting xenomicrobiota colonization. Front Microbiol 2017;8:1208.

[88] Taniguchi T, Miyauchi E, Nakamura S, et al. Plasmodium berghei ANKA causes intestinal malaria associated with dysbiosis. Sci Rep 2015;5:15699.

[89] Mooney JP, Lokken KL, Byndloss MX, et al. Inflammation-associated alterations to the intestinal microbiota reduce colonization resistance against non-typhoidal Salmonella during concurrent malaria parasite infection. Sci Rep 2015;5:14603.

[90] Denny JE, Powers JB, Castro HF, et al. Differential sensitivity to plasmodium yoelii infection in C57BL/6 mice impacts gut-liver axis homeostasis. Sci Rep 2019;9(1): 3472.

[91] Yilmaz B, Portugal S, Tran TM, et al. Gut microbiota elicits a protective immune response against malaria transmission. Cell 2014;159(6):1277–89.

[92] Jacobson A, Lam L, Rajendram M, et al. A gut commensal-produced metabolite mediates colonization resistance to salmonella infection. Cell Host Microbe 2018;24 (2):296–307 e7.

[93] Chakravarty S, Mandal RK, Duff ML, Schmidt NW. Intestinal short-chain fatty acid composition does not explain gut microbiota-mediated effects on malaria severity. PLoS One 2019;14(2):e0214449.

[94] Fried M, Kurtis JD, Swihart B, et al. Systemic inflammatory response to Malaria during pregnancy is associated with pregnancy loss and preterm delivery. Clin Infect Dis 2017;65(10):1729–35.

[95] Kabyemela ER, Muehlenbachs A, Fried M, Kurtis JD, Mutabingwa TK, Duffy PE. Maternal peripheral blood level of IL-10 as a marker for inflammatory placental malaria. Malar J 2008;7:26.

[96] Rogerson SJ, Pollina E, Getachew A, Tadesse E, Lema VM, Molyneux ME. Placental monocyte infiltrates in response to plasmodium falciparum malaria infection and their association with adverse pregnancy outcomes. Am J Trop Med Hyg 2003;68 (1):115–9.

[97] Neres R, Marinho CR, Goncalves LA, Catarino MB, Penha-Goncalves C. Pregnancy outcome and placenta pathology in plasmodium berghei ANKA infected mice reproduce the pathogenesis of severe malaria in pregnant women. PLoS One 2008; 3(2):e1608.

[98] Conroy AL, Silver KL, Zhong K, et al. Complement activation and the resulting placental vascular insufficiency drives fetal growth restriction associated with placental malaria. Cell Host Microbe 2013;13(2):215–26.

[99] Yooseph S, Kirkness EF, Tran TM, et al. Stool microbiota composition is associated with the prospective risk of plasmodium falciparum infection. BMC Genomics 2015;16:631.

[100] Scott JA, Berkley JA, Mwangi I, et al. Relation between falciparum malaria and bacteraemia in Kenyan children: a population-based, case-control study and a longitudinal study. Lancet 2011;378(9799):1316–23.

[101] Lokken KL, Mooney JP, Butler BP, et al. Malaria parasite infection compromises control of concurrent systemic non-typhoidal salmonella infection via IL-10-mediated alteration of myeloid cell function. PLoS Pathog 2014;10(5):e1004049.

[102] Mandal RK, Crane RJ, Berkley JA, et al. Longitudinal analysis of infant stool bacteria communities before and after acute febrile malaria and artemether/lumefantrine treatment. J Infect Dis 2018:jiy740. https://doi.org/10.1093/infdis/jiy740.

[103] Ravindran B, Satapathy AK, Das MK. Naturally-occurring anti-alpha-galactosyl antibodies in human Plasmodium falciparum infections—a possible role for autoantibodies in malaria. Immunol Lett 1988;19(2):137–41.

[104] Koren O, Goodrich JK, Cullender TC, et al. Host remodeling of the gut microbiome and metabolic changes during pregnancy. Cell 2012;150(3):470–80.

[105] Kho ZY, Lal SK. The human gut microbiome - a potential controller of wellness and disease. Front Microbiol 2018;9:1835.

[106] Nguyen QN, Himes JE, Martinez DR, Permar SR. The impact of the gut microbiota on humoral immunity to pathogens and vaccination in early infancy. PLoS Pathog 2016;12(12):e1005997.

[107] Desselberger U. The mammalian intestinal microbiome: composition, interaction with the immune system, significance for vaccine efficacy, and potential for disease therapy. Pathogens 2018;7(3).

[108] Waldman AJ, Balskus EP. The human microbiota, infectious disease, and Global Health: challenges and opportunities. ACS Infect Dis 2018;4(1):14–26.

[109] van Nood E, Vrieze A, Nieuwdorp M, et al. Duodenal infusion of donor feces for recurrent Clostridium difficile. N Engl J Med 2013;368(5):407–15.

[110] Konturek PC, Koziel J, Dieterich W, et al. Successful therapy of Clostridium difficile infection with fecal microbiota transplantation. J Physiol Pharmacol 2016;67(6): 859–66.

[111] Matuschewski K. Vaccines against malaria-still a long way to go. FEBS J 2017;284 (16):2560–8.

[112] Collado MC, Rautava S, Aakko J, Isolauri E, Salminen S. Human gut colonisation may be initiated in utero by distinct microbial communities in the placenta and amniotic fluid. Sci Rep 2016;6:23129.

[113] Yassour M, Jason E, Hogstrom LJ, et al. Strain-level analysis of mother-to-child bacterial transmission during the first few months of life. Cell Host Microbe 2018;24 (1):146–54 e4.

[114] WHO. World Malaria Report 2018. World Health Organization; 2018.